FMRI study of the brain correlates of hedonic and sensory perception during thermal alliesthesia

Marc-André Bacon

A Thesis

in

The Department

of

Psychology

Presented in Partial Fulfillment of the Requirements
for the Degree of Master of Arts at Concordia
University
Montreal, Quebec, Canada

June 2014

CONCORDIA UNIVERSITY

School of Graduate Studies

This is to certify that the thesis prepared

By: Marc-André Bacon

Entitled: FMRI study of the brain correlates of hedonic and sensory perception during thermal alliesthesia

and submitted in partial fulfillment of the requirements for the degree of

Masters of Arts (Psychology)

Complies with the regulations of this University and meets the accepted

standards with respect to originality and quality.

Signed by the final examining committee:

Dr. Nadia Chaudhri Chair

Dr. Virginia Penhune Examiner

Dr. Uri Shalev Examiner

Dr. Peter Shizgal Thesis Supervisor

Approved by Dr. Nadia Chaudhri
Chair of Department or Graduate Program Director

2014 Dr. Joanne Locke
Dean of Faculty

Abstract

FMRI study of the brain correlates of hedonic and sensory perception during thermal alliesthesia

Marc-André Bacon

This functional MRI experiment uses the alliesthesia phenomenon to map the brain correlates of hedonic experience and sensation. Alliesthesia refers to the dependence of the hedonic impact of a stimulus on the 'milieu interne'. Thus, a thermal stimulus applied to the skin during hyperthermia or hypothermia should be perceived as having the same temperature but opposite hedonic impact. Twenty participants took part in two successive scanning sessions during which mild states of hyperthermia and hypothermia were induced. Participants wore a water-perfused suit consisting of a long-sleeved shirt and trousers. In two of the stimulus conditions, either cold or hot water perfused the suit; in the third 'neutral' condition, water flow was interrupted. At intervals of 9 seconds, the participants rated, on two Likert scales, the thermal sensation perceived (from hot to cold) and the corresponding hedonic experience (from unpleasant to pleasant).Three different regressors were built from the ratings: hedonic, homeostatic, and sensory. The hedonic regressor was derived from the pleasantness ratings, whereas the sensory regressor was derived from the temperature ratings. The homeostatic regressor was also derived from the temperature ratings, but the sign was adjusted to conform to the value that would oppose the deviation of core temperature. Application of the hedonic and homeostatic regressors revealed conjoint activations in the more lateral areas of the orbitofrontal cortex. Application of the sensory regressor revealed clusters of

activation, mainly in the middle frontal gyrus, the superior frontal gyrus, the precentral gyrus, and the right orbitofrontal cortex.

Acknowledgements

The success of this research project was only possible with the involvement of many committed people. The first person I would like to thank is my supervisor, Professor Peter Shizgal. I could not ask for more from a supervisor; it was a privilege to work with him. Not only did he develop the experimental procedure (which I personally found ingenious) and supervised this complex research project, but he also supported me through difficult moments. I am really grateful for everything. I would like also to thank my colleague Brian Dunn and Dr. Kent Conover. Brian helped me at different levels, notably in the preparation and execution of the experiment. He was also generous with his time and advice, which simplified my task. As for Kent, among other things, he was extremely helpful with the data analysis. I was fortunate to benefit from his expertise. Moreover, I would like to thank him for his patience and for making himself available to me over the course of the project.

Our research team counted on six very professional assitants at different moments: Alexa Larouche Wilson, Meagan Barrett-Bernstein, Philip Desormeau, Karine Paquin, Vanessa Zappitelli, and Hannah Furby. They all played a crucial role in the execution of this experiment. At the technical level, I would like to thank David Munro and Christophe Lower who provided reliable experimental apparatus. We also benefited from the assistance of a great medical staff, formed by Dr. Gilles Plourde and Louise Ullyatt.

I also want to thank all the staff led by André Cormier at the McConnell Brain Imaging Centre of the Montreal Neurological Institute for their much appreciated help

throughout this experiment.

This research project was only possible with the financial support of the Canadian Institutes of Health Research.

Finally, I would like to thank my parents for their unfailing support. I want to dedicate my thesis to both of them, with a special thought to my dad who passed away on November 15, 2012. Merci pour tout papa!

Table of Contents

List of Figures

Introduction

After a long and exhausting trip, you are finally about to eat a favorite meal that you have been dreaming of, and the smell of that tasty dish makes your mouth water. You are enjoying every single bite, which is even better than expected, to a point where you can't control yourself. It is just so good … But by continuing eating beyond the moment you feel completely full, you will reach a state where even the smell of that delicious food will have become aversive. You have probably experienced this sensation at some point in your lifetime. This type of phenomenon was observed and explained first by Cabanac (1971) who called it alliesthesia. For Cabanac, alliesthesia refers essentially to the relation between the pleasure or the unpleasantness felt and the 'milieu interne' of an organism. In the previous example, the state of satiety changed the hedonic value of your favorite meal. In that sense, the phenomenon of alliesthesia has a strong motivational impact. For Cabanac, organisms are primarily driven by the search of pleasure and the avoidance of potential suffering. Three main types of primary reinforcers can procure pleasure according to Cabanac: chemical (odor, taste), mechanical (sex), and thermal (related to body core temperature). The latter is of particular interest. Within the context of thermal deviation (hypothermia or hyperthermia), pleasure would result from thermal stimulation that promotes a return to normothermia and thus fosters survival of the organism. Unpleasantness, on the other hand, would be caused by thermal stimulation that exacerbates thermal deviation. Interestingly, in both cases, the temperature of identical thermal stimulation (hot or cold) would be perceived similarly, but opposite hedonic values would be assigned. For instance, people soaking in hot tubs after freezing

in a cold winter day or after wilting on a hot summer day could have very different experiences.

The phenomenon of alliesthesia is a promising framework for distinguishing brain correlates of hedonic value from those of sensation. A few experiments in neuroimaging have been done specifically with non-noxious thermal stimulation, but none of the published work has yet fully exploited the potential of alliesthesia. We will review the previous studies by highlighting the main methodological differences and results.

In a functional magnetic resonance imaging (fMRI) experiment conducted by Rolls, Grabenhorst, & Parris (2008), thermal stimulation was applied on the dorsum and palm of the left hand of 12 participants with a thermode and a thermal resistor. A series of four different stimulations were delivered in a random permuted order: a warm pleasant stimulus, a cold unpleasant stimulus, and two distinct combinations of warm and cold stimuli with different degrees of pleasantness. Rolls, Grabenhorst, and Parris derived distinctive brain activations from correlations between the ratings of the participants (on pleasantness, unpleasantness, and stimulus-intensity scales) with the blood-oxygen-level-dependent (BOLD) signal. Activations in the mid-orbitofrontal cortex, the pregenual cingulate cortex, and the ventral striatum were associated with the positive hedonic state; activations in the lateral parts of the orbitofrontal cortex were related to the negative hedonic value. The intensity of the stimulation was correlated with the BOLD signal in the somatosensory cortex and the ventral posterior insula.

Using a different neuroimaging technique, Positron Emission Tomography (PET), Farrell et al. (2011) also investigated this specific question. Unlike the Rolls,

Grabenhorst, and Parris experiment, they stimulated the whole body with a water-perfused suit. Oral and skin temperatures were recorded. Notably, Farrell et al. relied on the latter to define a stable state (fixed at 34 degrees Celsius) for the establishment of five successive trials: 'neutral', cool, 'neutral', warm, and cool. These three different types of trials, resulting from the water temperature (set either at 4, 34, or 50 degrees Celsius) circulating through the suit, were administered to 12 participants lying in a scanner. Both the cool and the warm trials lasted for a period of 10 to 20 minutes, when the temperature of the skin had reached a stable state. During the experiment, the participants rated the intensity and pleasantness of the stimulation. We should specify that none of the scans were performed during the pleasant transitions. To determine the brain regions associated specifically with the hedonic valuation, Farrell et al. contrasted the latter with the correlates of the oral and the skin temperatures. They observed activation in the posterior part of the mid-cingulate cortex, which differed from the activation found by Rolls, Grabenhorst, and Parris in the lateral parts of the orbitofrontal cortex.

In a recent study, Dunn et al. (2010) performed a fMRI experiment that incorporates a significant modification : with a water-perfused suit, they induced a mild-state of hyperthermia and hypothermia before stimulating participants with a series of eight consecutive hot and cold water trials (135 sec per trial). Dunn et al. performed two scans per participant, one for each thermal state, using a similar experimental design to that of this current study (presented in the methods section). The order of the trials differed between each scan so that the initial trial of each series was designed to lead to an unpleasant feeling (hot – hyperthermia; cold – hypothermia). With this procedure, they mapped brain correlates of hedonic valuation. During the experiment, 16 participants

rated their hedonic and sensory perceptions. Based on the sensation perceived and the thermal state, a regressor ('homeostatic') was built to predict which thermal stimulation would be evaluated as pleasant or unpleasant (i.e., in hyperthermia, a hot thermal stimulation should be perceived as hot and unpleasant). An analysis of the brain activations common to the two thermal conditions showed similar results for both the hedonic and homeostatic regressors: activations in the ventromedial prefrontal cortex, the bilateral orbitofrontal cortices, the bilateral temporal poles, the bilateral superior and inferior temporal gyri, and the subgenual cingulate gyri. Further analysis revealed a distinct brain area that was particular to the hedonic regressor: the right medial orbital sulcus (located in the orbitofrontal cortex).

These results, at least the ones of Rolls, Grabenhorst, and Parris and Dunn et al., provide evidence for the primordial role played by the orbitofrontal cortex in hedonic valuation as established widely in the field of neuroscience (Kringelbach & Rolls, 2004; Kringelbach, 2005; O'Doherty, 2007; Murray, O'Doherty & Schoenebaum, 2007; Grabenhorst & Rolls, 2009; Grabenhorst & Rolls, 2011). Anatomically, this cortical area receives signals from the different sensory modalities, including the somatosensory cortex, and is reciprocally connected to several brain structures related to emotion and reward such as the amygdala, hippocampus, hypothalamus, striatum, and cingulate cortex (Kringelbach, 2005).

In the current fMRI experiment, we essentially set out to replicate the main results obtained by Dunn et al. Our experimental design differs only by the addition of a new condition in the sequence of trials: the 'neutral' trial in which no water flows. This new condition makes the predetermined sequence of trials less predictable for the participants

and thus, attenuates the probable effects related to the anticipation and learning processes. Also, the inclusion of neutral trials makes it possible, in principle, to distinguish between single- and dual-ended encoding of hedonic responses.

Methods

Participants

Twenty healthy young adults, aged between 19 and 33 years, have participated in this study (9 women and 11 men). The participants were mainly Concordia University students recruited on campus. Fourteen of them were from different sports teams. Two participants, who were not from Concordia University, were recruited after hearing about the experiment.

The data for three of these participants cannot be used in the current study. One participant (a male) withdrew from the experiment due to claustrophobia. Data from two other participants (one female and one male) were not usable. Technical difficulties occurred during the scanning process in the case of the female participant, and the hyperthermia condition of the male participant was not analyzed because he fell asleep in the scanner.

Screening procedures

All the participants underwent psychological and physical evaluations after having read and signed a consent form approved by the Montreal Neurological Institute and Hospital Research Ethics Board as well as the Concordia University Human Research Ethics Committee. The psychological screening consisted of a Structured Clinical Interview based on the DSM-IV-TR (American Psychiatric Association, 2000) and a questionnaire assessing depression (Beck Depression Inventory, Beck et al., 1961). The participants also filled out a magnetic resonance imaging screening form during that meeting. We were particularly vigilant regarding addictions (alcohol and drug of abuse),

current mood disorders or histories of mental illness and head injuries. Responsible, persevering, active young adults were the kind of participants we sought. Once selected, all the participants underwent a cardiac stress test overseen by the cardiologist, Dr. Marcel Fournier, at the Queen Elizabeth Health Complex in Montreal. This measure was taken to detect cardiac abnormalities that are risk factors for the performance of aerobic exercise.

Experimental sequence

Data from each participant was acquired over the course of day, and included two thermal-induction periods, one to produce hyperthermia and one to produce hypothermia, each followed by a scanning session. The day began at 7:30 AM at the McConnell Brain Imaging Centre of the Montreal Neurological Institute (MNI) with a screening procedure consisting of a drug of abuse test (a QuickTox® dip card) and a pregnancy test for the females. Each participant also completed a questionnaire assessing affective mood state fluctuation (Profile of Mood States standard, McNair et al., 1992), a magnetic resonance imaging screening form, and a consent form. At 8:00 AM, after the participant donned the tube suit, we did a preliminary scan (about 10 seconds in duration) that had three purposes: to facilitate the acclimatization of the participant to the scanner environment, to test the head-stabilization procedure and to check our equipment. At that time, we also carefully explained the task to the participants. Next, a fiber-optic temperature probe was taped to the skin of the participant, between the second and third ribs, and preparations for the initial deviation of core temperature ensued.

The thermal-induction procedures were aimed at producing a one-degree Celsius deviation from the measured baseline at the start of the first thermal-induction period.

This baseline and the consequent deviation were measured with both an oral and a tympanic thermometer.

Hyperthermia was induced by the performance of aerobic exercise (pedalling a stationary bicycle) while wearing insulating clothing as hot water flowed through the tube suit. Throughout the deviation of core temperature, the participants held a modified snorkel mouthpiece in their mouths. This helped stabilize oral temperature while providing an access port for the oral thermometer.

By around 10:30 AM, the participant was generally ready to proceed with the first scan. As they experienced a series of predetermined thermal stimuli through their tube suits, the participants had to rate, continuously, their sensations and hedonic-state evaluations on two distinct scales presented in alternate order. Once the data was acquired, we started the second thermal induction. Hypothermia was induced by exposure to a cool environment while cold water flowed through the tube suit. When necessary, ice packs were placed in the axillae to speed the development of hypothermia. In the scanner, the participants again rated their thermal sensations and hedonic state. We finalized the data acquisition by 1:30 PM. After a snack and shower, the participants again completed the Profile of Mood States questionnaire and were debriefed. To ensure the safety of the participant, a registered nurse (Louise Ullyatt) was present and an anesthesiologist (Dr. Gilles Plourde) was on call throughout the thermal-induction and scanning periods.

Thermal control

The participant wore a water-perfused suit (Med-Eng Systems COOLTUBE Suit) consisting of a long-sleeved shirt and trousers (Figure 1). About 200-275 feet of 0.097''

Figure 1. Tube suit in detail.

ID Tygon tubing were sewn into the fabric in a serpentine pattern, thus allowing us to cool or heat the participant. Modified Gaymar MediTherm II hypo/hyperthermia units served as the sources of hot and cold water; two backup units were kept on hand and at the target temperatures. For both the thermal inductions and the scanning sessions, the set points for the cold and hot water were at 10 and 52 degrees Celsius, respectively. Due to their ferromagnetic components, the MediTherm II units had to be placed outside the Faraday shield in the machine room adjacent to the scanner enclosure. A pair of booster pumps, also housed in the machine room, provided the pressure/flow characteristics required to produce adequate flow in the suit-perfusion circuit. Insulated dual-channel hoses, 25 feet in length, were passed through the Faraday shield so as to link the outputs of the booster pumps to a specially designed MRI-compatible valve, which was positioned next to the scanner during the experiment. The proximity of the valve to the participant minimized the delays entailed in changing the suit temperature. To complete the circuit represented in Figure 2, an additional 10-foot, dual-channel hose, connected

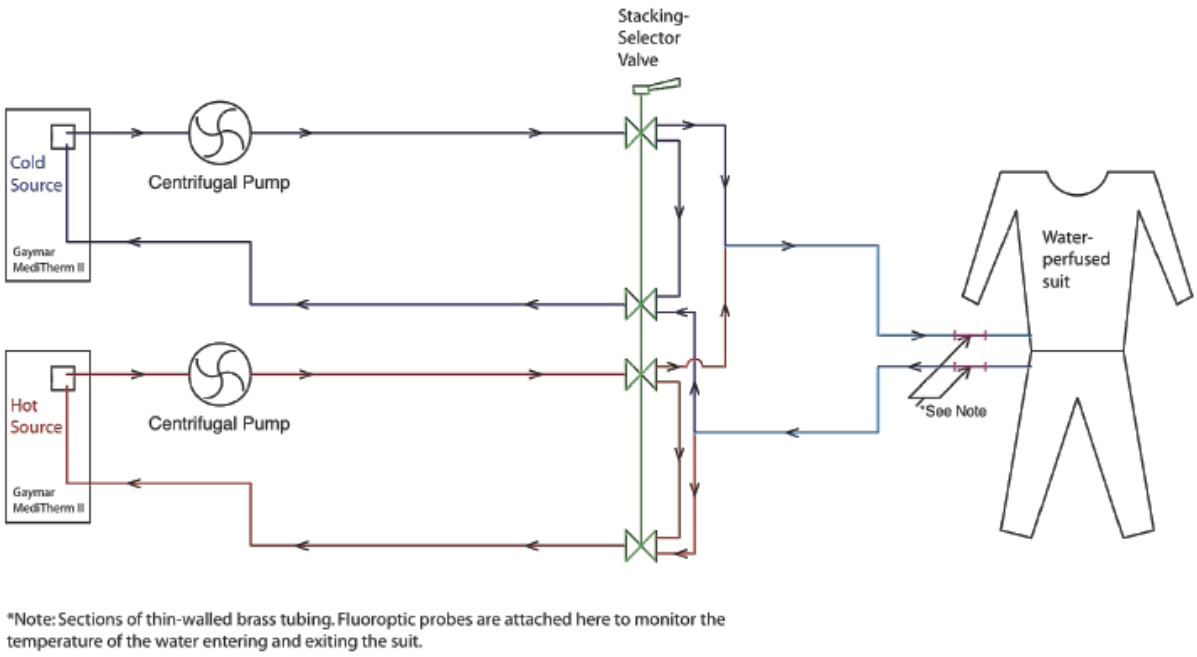

Figure 2. Thermal control schematic.

the valve to the tube suit worn by the participant.

Three different flow conditions were in force during the scanning session, each determined by appropriate positioning of the valve handle. During the 'cold' condition, water from the cold source flowed through the suit, during the 'hot' condition, water from the hot source flowed through the suit, and during the 'neutral' condition, no water flowed through the suit. Throughout the scanning session, a team member operated the valve according to a predetermined sequence presented on a digital display.

Temperature monitoring

During the induction of both the hyperthermic and hypothermic states, we measured the core temperature of the participants every three minutes with an oral thermometer (Welch Allyn SureTemp Plus 690, Skaneateles Falls, NY) and a tympanic thermometer (Braun ThermoScan Pro 4000, Skaneateles Falls, NY). Once the target

temperature had been achieved and the participant had been transferred to the anteroom of the scanner, the mouthpiece was exchanged for one that included a port for a temperature-sensitive fiber-optic probe. This sensor, the skin sensor, and sensors positioned to monitor the temperature of the water entering and exiting the suit were connected, via fiber-optic patch cords that passed through the Faraday shield, to a biomedical fluoroptic thermometry system (model 3100, Luxtron, Santa Clara, CA), thus allowing us to obtain temperature readings while the subject was in or near the scanner.

Thermal inductions

Hyperthermia was induced by performance of mild aerobic exercise while hot water flowed through the suit. To facilitate the induction of hyperthermia, each participant wore fleece garments (top and bottom), a waterproof Tyvek jumpsuit (which served as an evaporation barrier), a fleece neck tube, a pair of insulated gloves, and a tuque over the tube suit (Figure 3). Once hot-water flow was established (the water reaching the suit was about 48 degrees Celsius), the participant started to pedal a stationary bicycle at a speed of ~15 km/h with a limited load. The induction was generally achieved after 45-60 minutes.

Prior to induction of hypothermia, the insulating clothing was removed. Cold water was then pumped through the suit while the participants slowly pedalled the stationary bicycle, which was located in a cool environment (the machine room). The purpose of the slow pedalling was to facilitate exchange of cooled blood from the periphery with the body core due to the rhythmic contraction and relaxation of major muscle groups. Roughly 45-60 minutes were required to reach the target core temperature.

Figure 3. Participant during the hyperthermia induction.

Experimental design

A similar experimental design was used for the scanning sessions conducted during hyperthermia and hypothermia (Figure 4). The block design consists of a series of 12 trials (including two dummy trials, one at the beginning and the other at the end). The trial sequences for the hyperthermic and hypothermic conditions were inverted in terms of the temperature of the water flowing through the suit but were intended to be congruent hedonically. For example, hot water flowed through the suit in the hyperthermia condition and cold water during the hypothermia condition. Cabanac's alliesthesia theory predicts that both of these flow conditions would be experienced as unpleasant**.** The entire sequence of intended hedonic states is as follows: bad (dummy), bad, good, bad, neutral, good, neutral, bad, good, bad, neutral, neutral (dummy). The duration of each hot- and cold-water trial (except for the dummy trials) was 126 sec (or

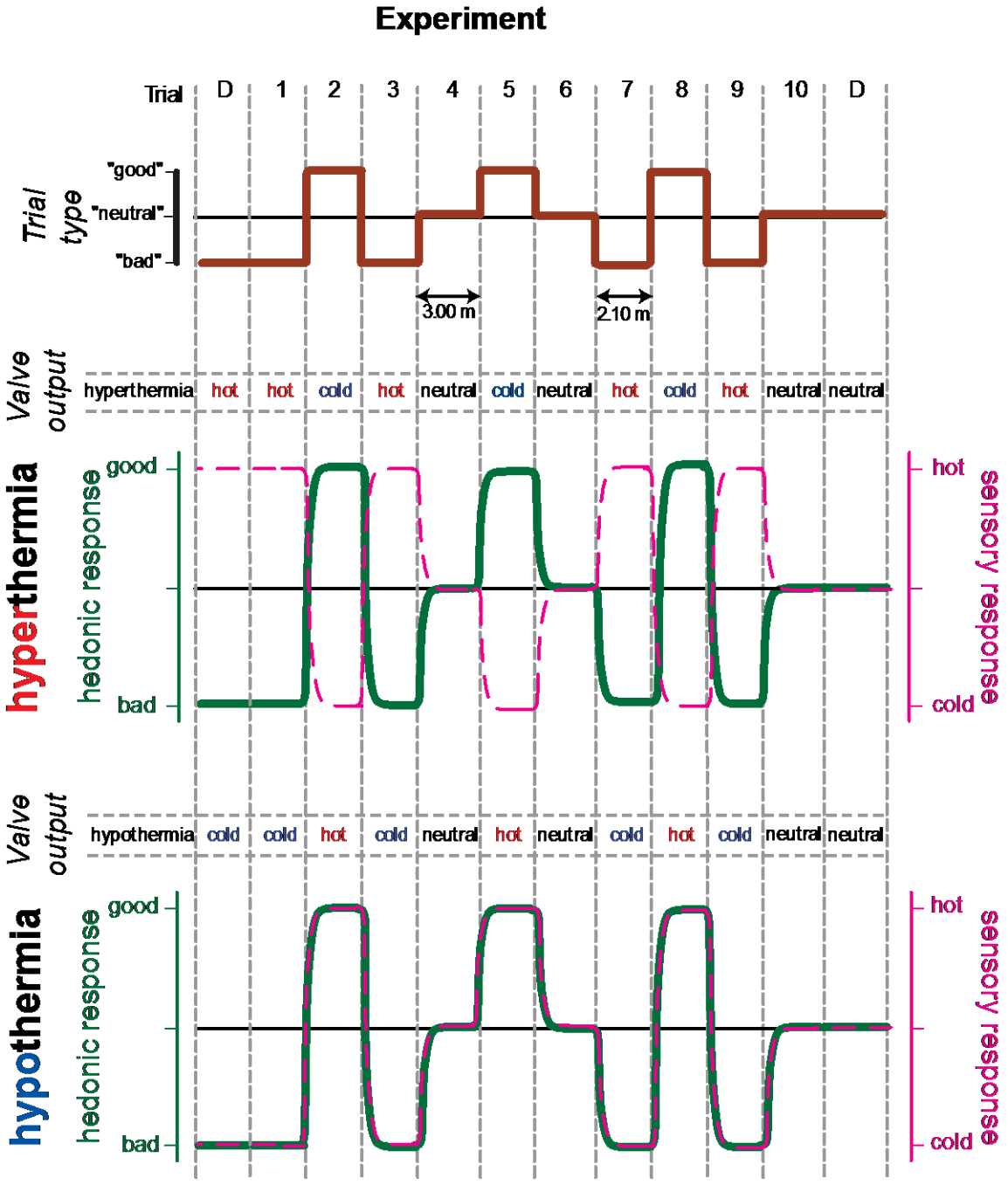

Figure 4. Experimental design schematic.

56 repetition times (TRs), which represents the time to acquire a complete set of 'slices' spanning the targeted brain volume (2.25 sec)); whereas the duration of each neutral trial was 180 sec (or 80 TRs). The reason for longer neutral trials was to allow the body to bring the temperature of the still water in the tubing closer to skin temperature, thus producing an 'indifferent' hedonic state (neither pleasant nor unpleasant).

Throughout the trial sequence, the participants rated their hedonic state and thermal sensation. Alternating Likert scales were projected for nine seconds on a screen visible via a mirror on the headcoil. One scale depicted a hedonic continuum ranging from unpleasant (-5) to pleasant (+5), whereas the other depicted thermal sensations ranging from cold (0) to hot (10).

Regressors

From the hedonic and sensory ratings, we derived three distinct regressor sets: hedonic, sensory, and homeostatic. As their names imply, the purpose of the hedonic and sensory regressors is to identify brain regions in which the BOLD signal is correlated with the ratings. The purpose of the homeostatic regressors is to identify brain regions in which the BOLD signal is correlated with the potential of the thermal stimulation to re-establish normothermia (i.e., to move core temperature back towards its set point). The homeostatic regressor was thus derived from the sensory ratings. For example, a rating of 'hot' on the sensory scale during hyperthermia is assigned a negative homeostatic value because the water flow that generates this sensation will accentuate the deviation of core temperature from its set point. Similarly, a rating of 'cold' on the sensory scale during hyperthermia is assigned a positive value because the water flow that generates this sensation will reduce the deviation from set point. Thus, the homeostatic regressor

consists of the inverse of the sensory ratings obtained during hyperthermia and the non-inverted sensory ratings obtained during hypothermia. Perfusion of the suit with hot water, which generates positive ratings on the sensory scale, accentuates the deviation of core temperature during hyperthermia but reduces it during hypothermia.

The button box used to register the ratings was sampled at a rate of 1 Hz. By means of interpolation, the resulting vector was downsampled to the frame rate of the scan acquisition (i.e., to generate one rating for each TR). The final rating in each 9-second rating epoch was used to construct the regressors (Figure 5). The rationale for this practice is that the adjustment in the ratings occurred almost exclusively during the early portion of the 9-second epoch, and the ratings were generally stable for the remainder. Finally, each of the three regressors was normalized so as to vary between 0 and 1.

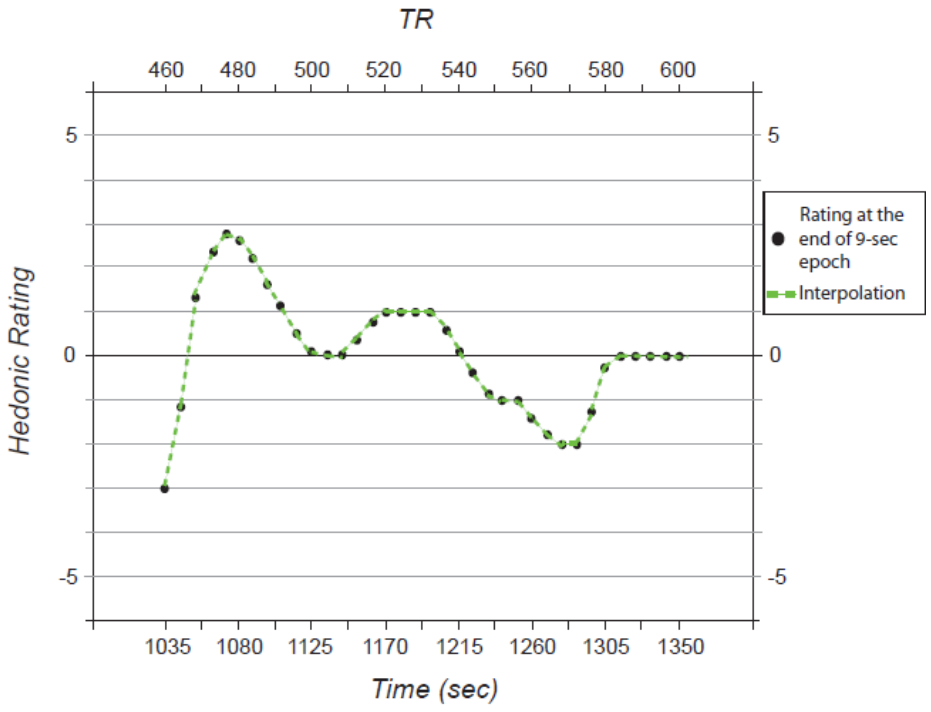

Figure 5. Section of the hedonic ratings obtained from one participant and interpolation to build the regressor.

Scanning

The brain images were acquired using a 3-Tesla Siemens Magnetom Trio scanner with a 32-channel head coil. A series of scans was performed for each thermal condition in this order: AA Scout, localizer-TruFisp, functional scan, GRE field-mapping scan, and high resolution structural scan. The AA Scout, as described by the Center for Brain Science of Harvard University, 'takes two low-resolution whole-head scans, and compares the result to a brain atlas on the scanner. This is used to position all future scans in the session, and ensure reproducible positioning if the subject is scanned multiple times.' TruFisp registers imaging sequences to anatomical landmarks. For the functional scan, gradient echo EPI sequences generated the T2* weighted images with blood oxygenation level-dependent (BOLD) contrast. We used the following acquisition parameters: Field of view = 256 mm, TE = 30 msec, TR = 2.25 sec, Flip angle = 90˚, voxel size = 4x4x4 mm. A total of 664 volumes (36 slices per volume) for each condition were acquired using an interleaved acquisition order at an angle of 30˚ from the anterior commissure-posterior commissure line to reduce the susceptibility effects due to the proximity of the sinuses to the orbitofrontal cortex (Deichmann et al., 2003). The GRE field-mapping scan also helps correct for susceptibility effects. The spatial distortions (functional signals from places close to the sinuses that are artifactually displaced) can be corrected given a map of the B0 field distortion that is derived from the GRE field-mapping scan. Finally, the structural scans were 3D T1-weighted images with a voxel size of 1 mm^3.

Data analysis: Preprocessing and registration

The analyses were performed with FSL library tools (FMRIB, Oxford, UK) executed under the control of a MATLAB (Mathworks, Natick, MA) script written by Dr. Kent Conover. Preprocessing began with motion correction, B0 field distortion correction, temporal filtering and spatial smoothing. The Motion Correction FMRIB's Linear Image Registration Tool (MCFLIRT) realigns the acquired volumes to the middle volume (Jenkinson et al., 2002) using 6 degrees of freedom (3 rotations and 3 translations). The correction of the field distortion was done using the field maps provided by the Siemens mapping protocol. A high-pass temporal filter was used to eliminate a range of frequencies lower than the ones of interest, determined by the repetition frequency of the experimental task ($2.5x10^{-3}$ Hz). A spatial Gaussian filter kernel of 5 mm full width half-maximum was also applied.

We used the Multivariate Exploratory Linear Optimised Decomposition into Independent Components (MELODIC) tool (Beckmann & Smith, 2004) to reduce systematic noise by revealing characteristic artifacts in data sets. By inspecting the spatial map and the corresponding time course of each component signal, this tool made it possible to identify and remove noise associated with head motion and slice drop-out. For this study, two independent raters reviewed the components for the appearance of these two specific artifacts. Components that were classed as noise by both raters were removed from the data. We finalized the preprocessing of the functional images by removing the first 16 volumes from each of the two data sets. This procedure was necessary considering the BOLD signal at time t reflects brain events as long as 18 sec (8 TRs) in the past due to the duration of the hemodynamic response. To make possible the

inclusion of response lags in the analysis, we started acquiring data 36 sec (16 TRs; 2.25 sec per TR) prior to the start of the first trial.

The anatomical images were first registered to a standard space (MNI 152 non-linear 1mm) using the FMRIB's Linear Image Registration Tool (FLIRT) and 12 spatial degrees of freedom (3 rotations, 3 translations, 3 scalings, and 3 skews), after separating each brain from the head using the Brain Extraction Tool (BET V2, Jenkinson, Pechaud & Smith, 2005). The preprocessed functional images were then registered, with the same tool, to their respective registered anatomical images. In those two cases, the spatial transformation was based on 12 degrees of freedom (3 rotations, 3 translations, 3 scalings, and 3 skews). The validity of the transformations was confirmed by comparing the warped anatomical images to the non-linear MNI 152 atlas.

Afterwards, we calculated the deformation fields (or warps) of the registered anatomical images based on the MNI 152 non-linear 1mm atlas, with the FMRIB's Non-linear Image Registration Tool (FNIRT) and applied the deformation fields to the corresponding functional images.

Data analysis: Model testing

The statistical analyses were based on the general linear model. At the subject level, the FMRI Expert Analysis Tool (FEAT) performs time series analysis using the FMRIB's Improved Linear Model (FILM). This tool allows correction for temporal autocorrelation for each single voxel of the preprocessed functional images. This correction is relevant only if the autocorrelation is estimated accurately, which necessitates spatial smoothing of the initial estimations (Smith et al., 2004). Removing the autocorrelation provides the best linear unbiased estimates of the three regressor sets

(Smith et al., 2004).

We also defined seven confounding variables for the analysis at the subject level: six motion parameters (3 rotations and 3 translations) and the volume mean time course. The latter, which is the series comprised of the mean BOLD signal arising from the brain in each functional volume, attempts to account for systematic noise sources (e.g., scanner drift) that contribute to the BOLD signal. Before proceeding to the regressions of the observed signals *per se* (two regressions per participant, one for each thermal state), we convolved the three regressor sets with a canonical gamma function to model hemodynamic responses. After estimating the regressors, we obtained six statistical maps (three regressors X two thermal conditions) for each participant, which correspond to the significant activations associated with each regressor set.

Using those statistical maps, we performed six distinct group analyses, one for each regressor and thermal state, with the FMRIB's Local Analysis of Mixed Effects (FLAME) tool (Beckmann, Jenkinson & Smith, 2003; Woolrich et al., 2004). Based on a Bayesian approach, this tool generates t-statistics describing activity in each voxel. FLAME generates an estimation of the unknown variances (and thus of the covariances) with the maximum *a posteriori* method. To obtain a more accurate estimation of the brain activity (reflected by the estimated parameters at the group level), each voxel near the significance threshold was then re-analyzed with the Markov chain Monte Carlo method. All the resulting t-statistics were then converted into z-scores afterwards. The FLAME tool also permits the detection and the de-weighting of outliers to improve the estimations.

Conjunction analyses

Identification of regions with common brain activity for both thermal states was performed via spatial conjunction analysis using MATLAB for each of the three regressors at the group level. We first looked at all the voxels in the statistical map of each thermal state, for the same regressor, which showed significant activity. We then retained only the voxels, located at the same spatial position, presenting statistically significant activity in both thermal states. The three conjunction maps obtained were overlaid on the non-linear MNI 152 template for anatomical localization.

Results

Behavioural results

We first evaluated the ratings of the participants, on both the hedonic and the perceived sensory scales for each of the two thermal conditions. The ratings were plotted against the series of thermal stimulations. Figures 6 and 7 show the results from two participants. The three different traces (blue, red, and grey) respectively reflect the ratings (hedonic or sensory), the temperature of the water reaching the suit, and the trial sequence. Recall that according to the theory of alliesthesia, the flow of hot water should be perceived as unpleasant when hyperthermic and pleasant when hypothermic; the flow of cold water should be perceived as pleasant when hyperthermic and unpleasant when hypothermic. These predictions are borne out fairly well by the results shown in Figure 6 (with the exception of the final 'hot' trial) and less well by the results from the hypothermia condition in Figure 7. The sensory ratings conform fairly closely to the temperature of the water entering the suit.

To achieve a better understanding of the ratings, we also conducted a principal component analysis (PCA). This mathematical technique was applied to assess the concordance of the ratings across subjects. The first principal component identifies the amount of rating variance that is common to all subjects, and the greater this amount is as a proportion of total variance, the more the subject ratings are intercorrelated. Concordance of individual ratings to the first principal component is indicated by a loading factor. Ratings that load positively on the first component are positively correlated with it, while those with negative loadings are negatively correlated.

Hedonic ratings – Hyperthermia

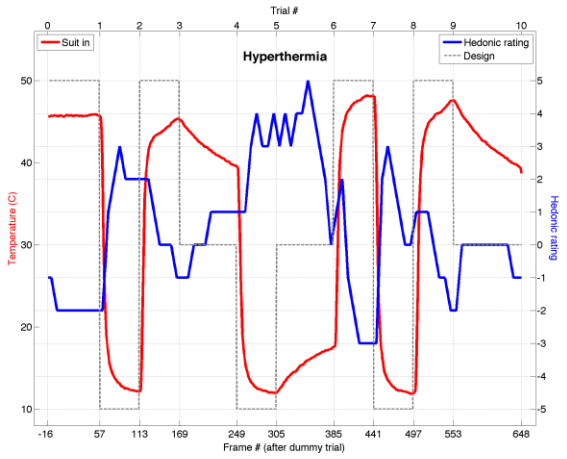

Sensory ratings – Hyperthermia

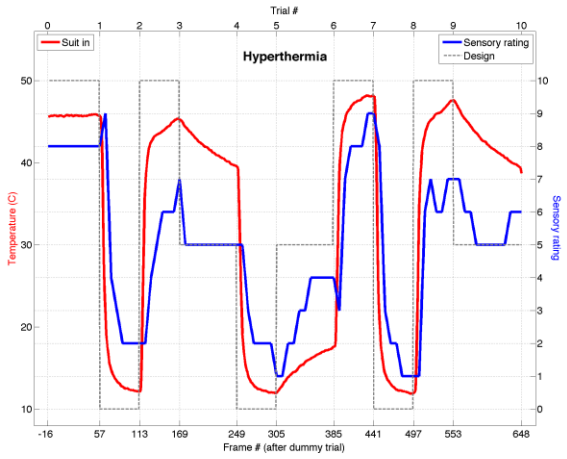

Hedonic ratings – Hypothermia

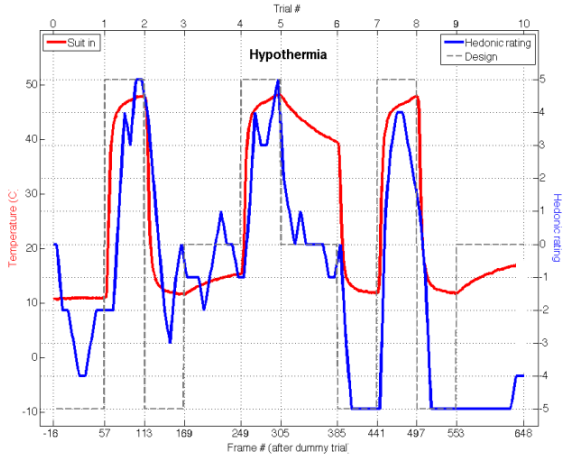

Sensory ratings – Hypothermia

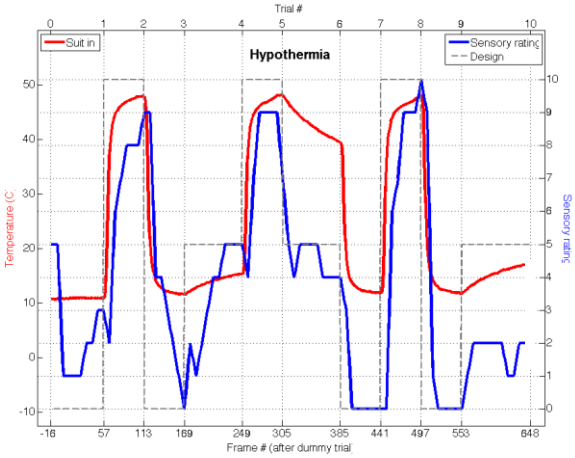

Figure 6. Plots of the ratings, for each thermal condition, against the series of thermal stimulations – case of participant (he111014) who rated in accordance to the alliesthesia predictions.

Hedonic ratings – Hyperthermia

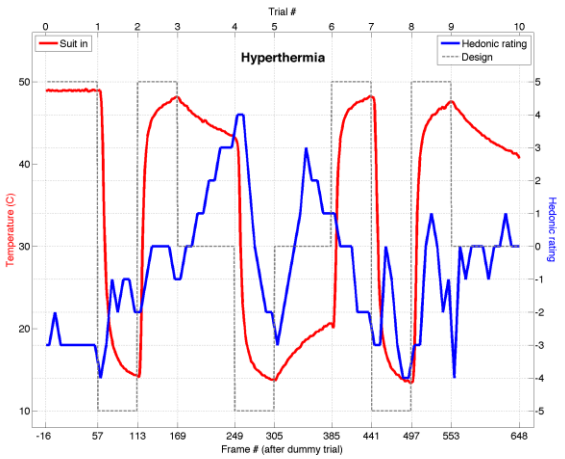

Sensory ratings – Hyperthermia

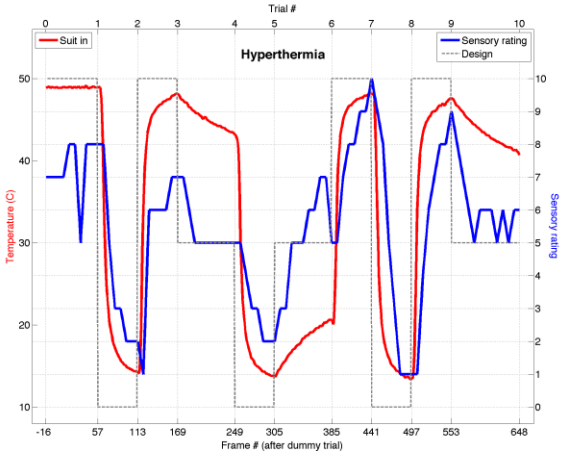

Hedonic ratings – Hypothermia

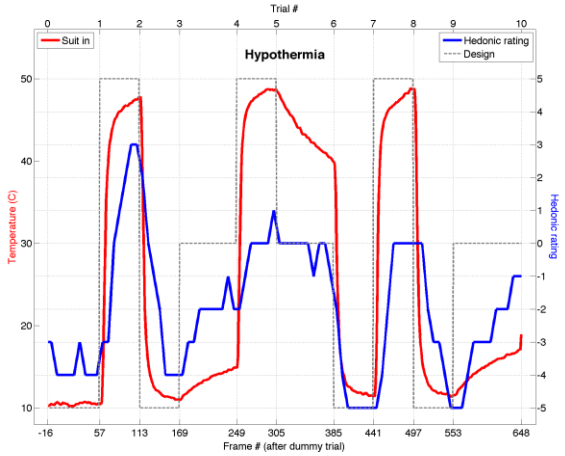

Sensory ratings – Hypothermia

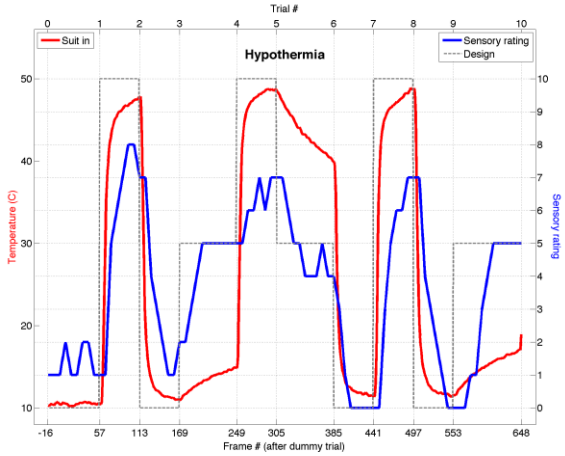

Figure 7. Plots of the ratings, for each thermal condition, against the series of thermal stimulations – case of participant (he120413) who rated to a lower degree of accordance to the alliesthesia predictions.

Ratings with small load factors are independent of the first component.

For each of the three regressor types (the homeostatic regressor differed from the sensory regressor only by the inversion of the sensory ratings for the hyperthermia condition), we first plotted the first principal component of each participant's normalized ratings against the scanning time expressed in TRs (Figure 8). The blue and red traces respectively represent the principal component and the predicted hedonic state. We can distinguish the different transitions reflecting our experimental design for each regressor type. We noticed the progressive return toward 'neutrality' in each of the three neutral trials. Interestingly, for the two neutral trials following a bad trial, the first principal component revealed that the ratings were slightly below the 'neutrality' level, whereas opposing results were observed in the neutral trial following the good trial.

We also generated heat maps reflecting the actual ratings of all the participants in both thermal conditions, as well as individual loadings for the first principal components (Figures 9, 10, and 11). In the heat maps, the ratings are expressed by the designated colour (blue through white through red) to represent the degree of pleasantness (bad-neutral-good) or the sensation perceived (cold-neutral-hot) during the trial sequence. The individual loadings, once multiplied by the first principal component, allowed us to recover the participants' ratings. The blue bars indicate the value of the loading for each participant. As becomes apparent when considering the heat maps and the individual loadings, a certain level of inconsistency is apparent only for the hedonic regressor in the hyperthermia condition. Four of the seventeen participants didn't rate as expected (Hyper_he110718; Hyper_he110822; Hyper_he120203; and Hyper_he120413).

First principal component for the hedonic regressors

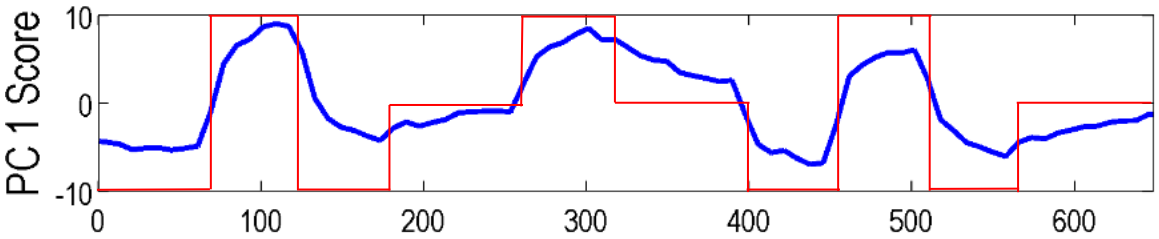

First principal component for the homeostatic regressors

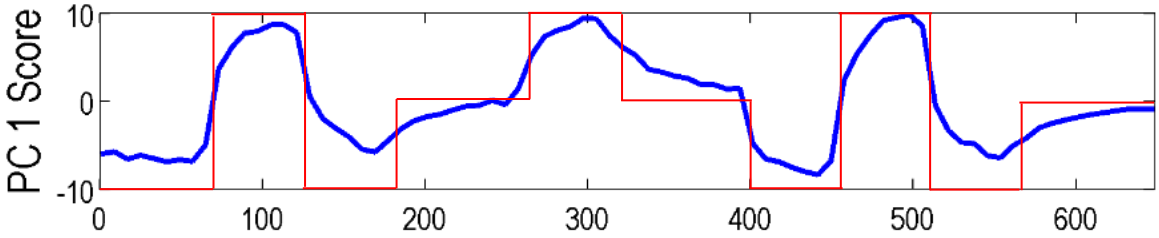

First principal component for the sensory regressors

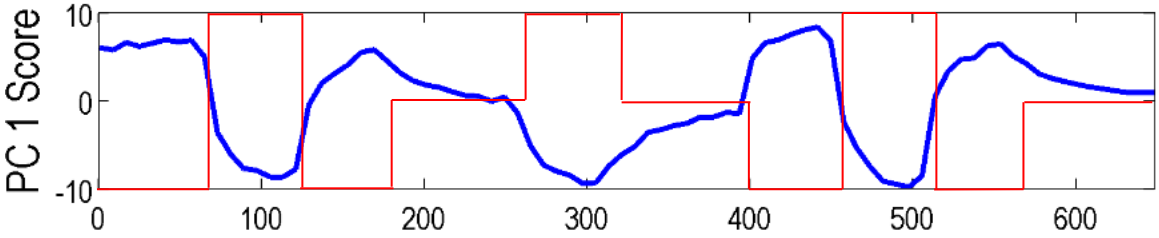

Figure 8. Plots, for each regressor type, of the first principal component of each participant's normalized ratings against the scanning time expressed in TRs.

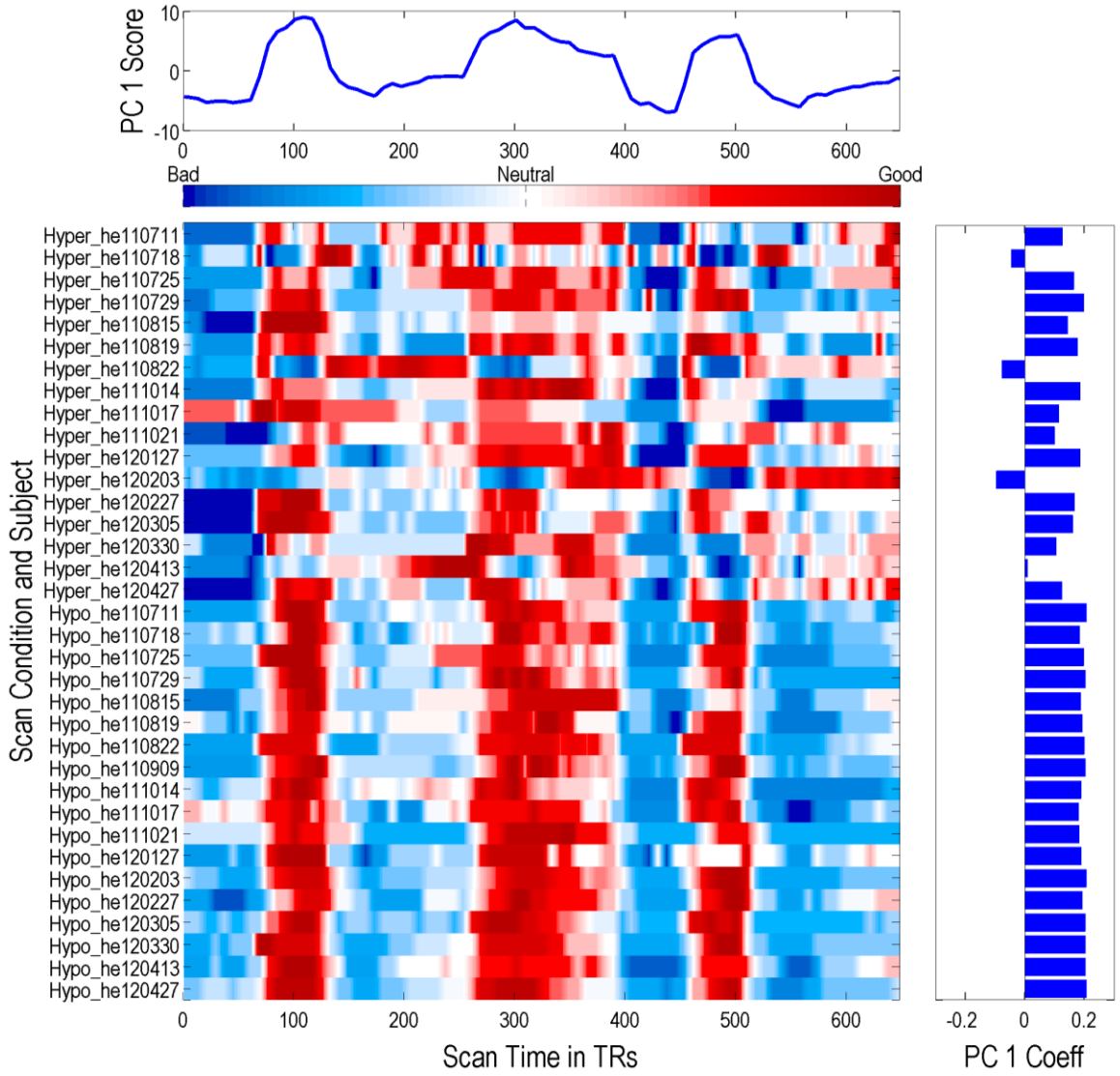

Figure 9. Heat map and individual loadings for the first principal component – hedonic regressor.

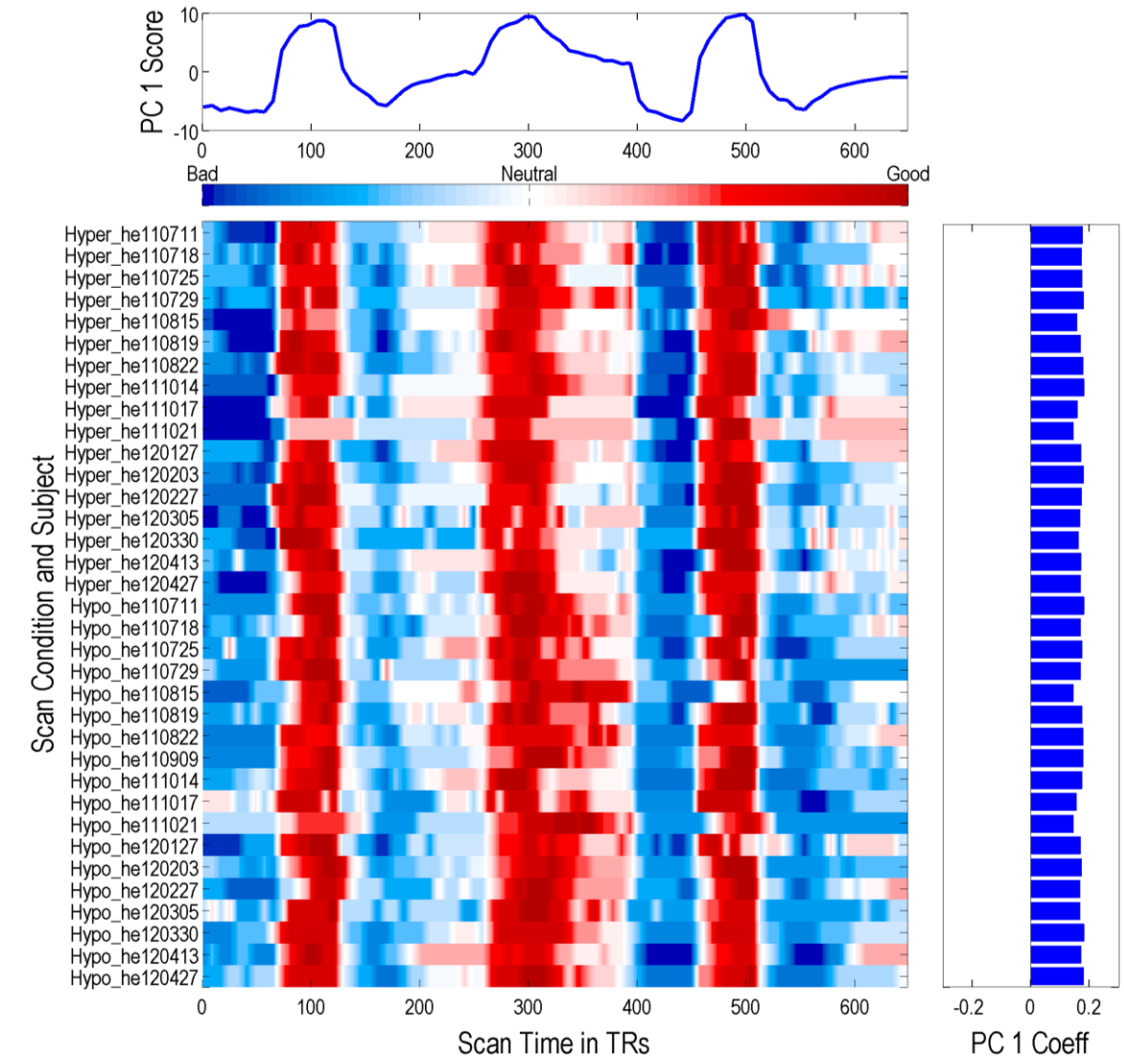

Figure 10. Heat map and individual loadings for the first principal component – homeostatic regressor.

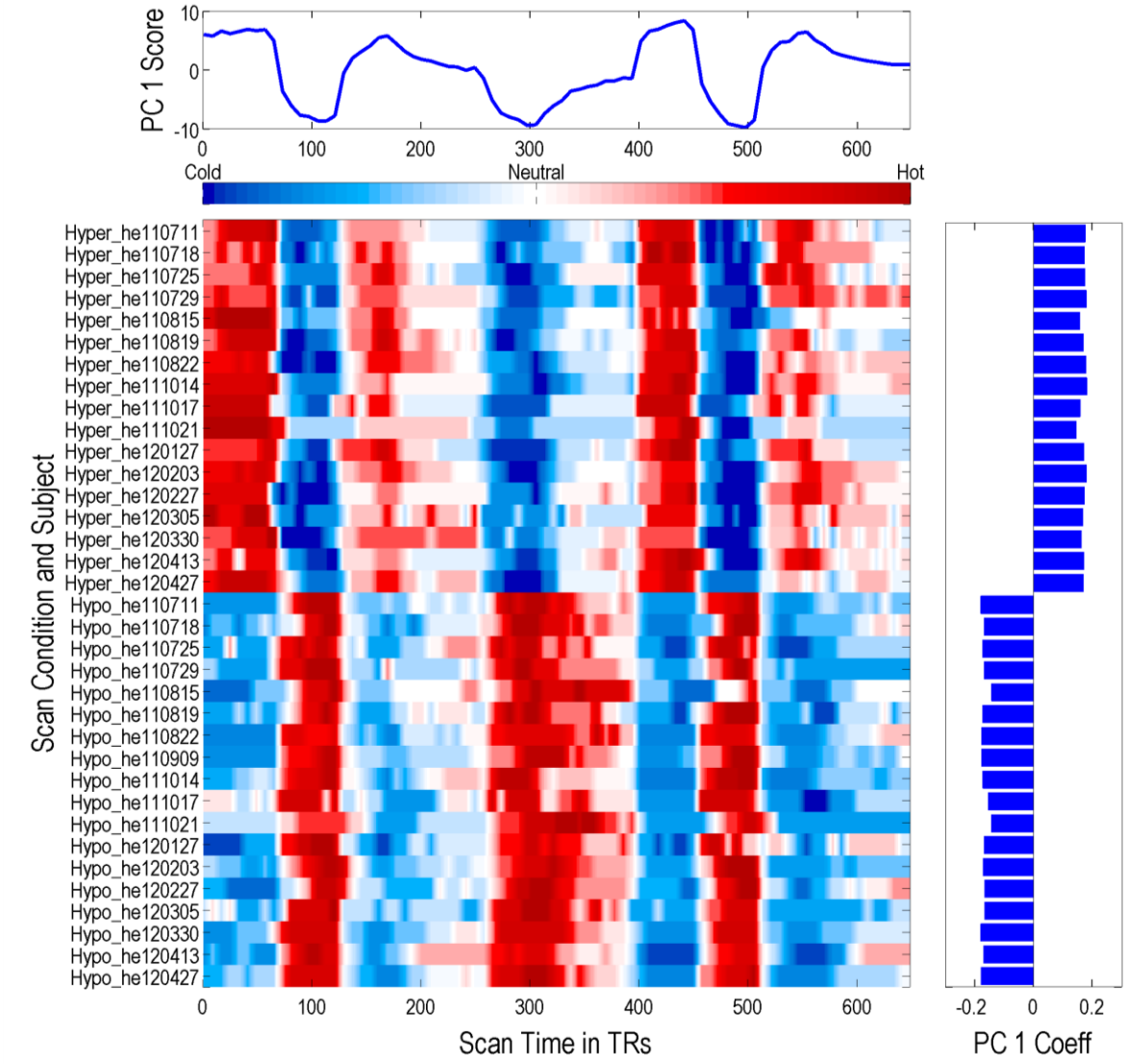

Figure 11. Heat map and individual loadings for the first principal component – sensory regressor.

fMRI results

Conjoint analysis

To identify both positive and negative BOLD signal correlates in the brain, in both thermal states for each of the three regressors, we conducted a conjoined analysis of the six corresponding statistical group maps. These specific regions are represented by the green clusters in the following figures. For the hedonic regressor, we presented in Figure 12 the conjoint positive correlation between the hyperthermia (in red) and the hypothermia (in blue) conditions. We observed two principal clusters, both in the more lateral parts of the orbitofrontal cortex (Peaks: x, y, z, Z-value = 23, 18, -25, 4.64; cluster size = 3123 mm^3 and x, y, z, Z-value = -25, 43, -19, 4.43; cluster size = 1338 mm^3). More precisely, following the cytoarchitectonic map of the orbitofrontal cortex established by Kringelbach (2005), the overlapping regions in the right hemisphere corresponded to parts of 11l, 11m, 131, and 13m. As for the left hemisphere, the positive correlation observed corresponded to parts of the regions 11l, 13l, and 47/12m (Figure 13). Smaller clusters were also observed, notably in the left frontal pole (Peak: x, y, z, Z-value = -43, 49, 22, 2.97; cluster size = 1121 mm^3) and in the subcallosal cortex (Peak: x, y, z, Z-value = -9, 19, -10, 3.37; cluster size = 452 mm^3), in keeping with the Harvard-Oxford Cortical Structural Atlas provided by FSL. We also compared our results for the hedonic regressor with the conjoint regions obtained in Dunn et al.'s study (presented in pink in Figure 14). On Kringelbach's map, we identified three clear regions in the orbitofrontal cortex in the right hemisphere: 11l, 11m, and 13m. In the left hemisphere, the three regions observed are limited to the border of the two clusters: parts of 11l, 13l, and 13m. Dunn et al.'s clusters are more medial than those in the current experiment.

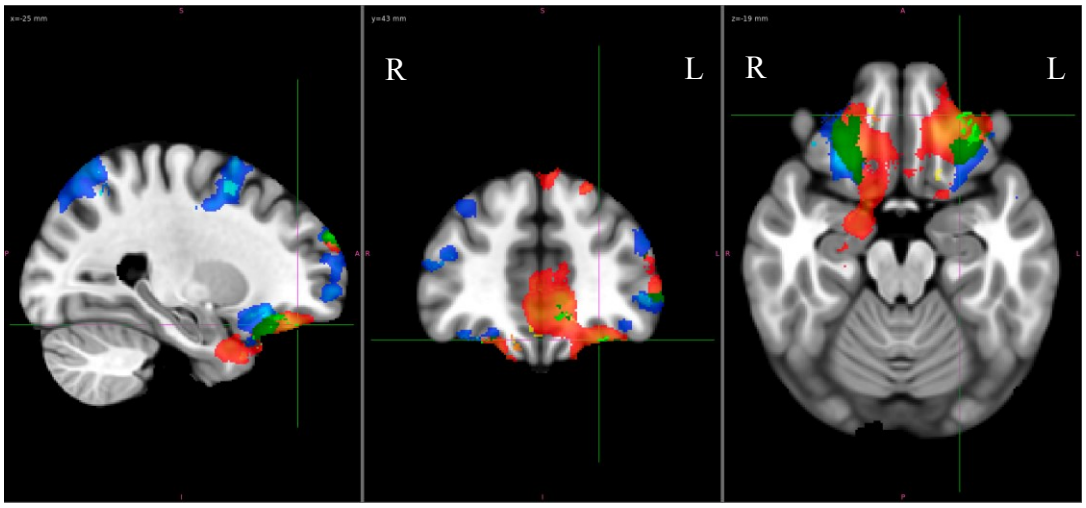

Figure 12. Conjoint analysis – positive BOLD signal correlates for the hedonic regressor. In blue: Hypothermia; in red: Hyperthermia; in green: Conjoint regions.

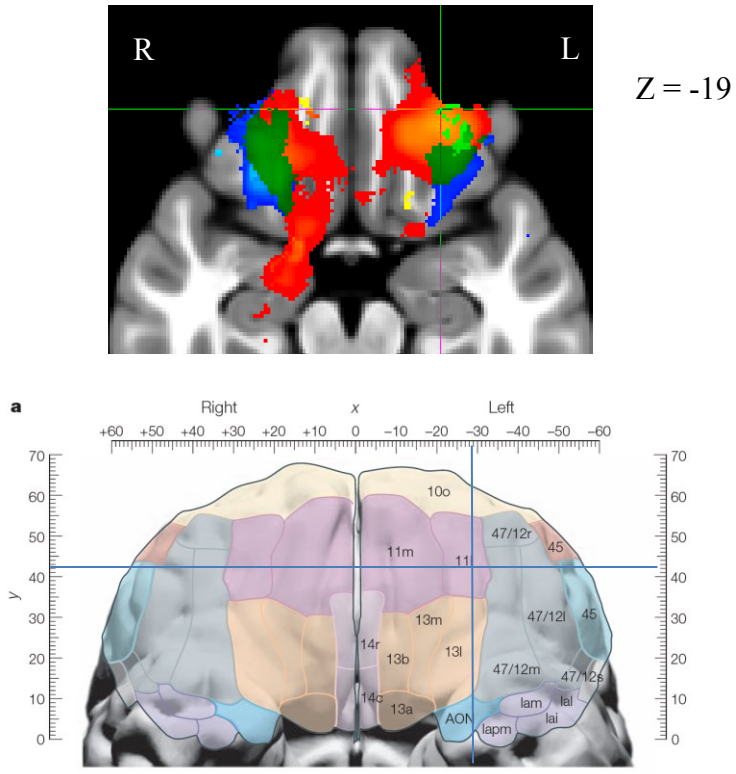

Figure 13. Localization of the orbitofrontal cortex hedonic correlations with the cytoarchitectonic map established by Kringelbach (2005).

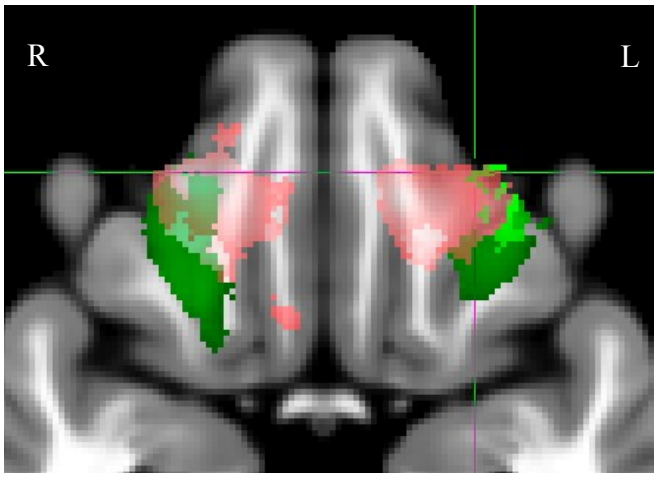

Figure 14. Conjoint analysis – comparison with Dunn et al.'s results for the hedonic regressor. In green: Conjoint regions; In pink: Conjoint regions in Dunn et al.'s study.

The negative correlates of the hedonic regressor reveal different conjoint regions. Among these conjoint regions, we found the precentral gyrus (Peak: x, y, z, Z-value = -19, 25, 67, 5.06; cluster size = 91 047 mm^3) and the cingulate gyrus (Peak: x, y, z, Z-value = 23, -47, 11, 3.54; cluster size = 715 mm^3) at the cortical level, and the right hippocampus (Peak: x, y, z, Z-value = 25, -22, -9, 2.90; cluster size = 60 mm^3) at the subcortical level (Figure 15).

In the case of the positive correlates of the homeostatic regressor, Figure 16 shows two main common clusters in the orbitofrontal cortex that overlap in the hyperthermia and the hypothermia conditions (Peaks: x, y, z, Z-value = 17, 45, -18, 4.49; cluster size = 3670 mm^3 and x, y, z, Z-value = -26, 39, -18, 4.59; cluster size = 2789 mm^3). We found a region corresponding to parts of 11l, 11m, 13l, and 13m in the right hemisphere. In the left hemisphere, the conjoint cluster overlapped parts of 11l, 13l, 13m, and 47/12m (Figure 17). We also see conjoint clusters in the left temporal pole (Peak: x, y, z, Z-value

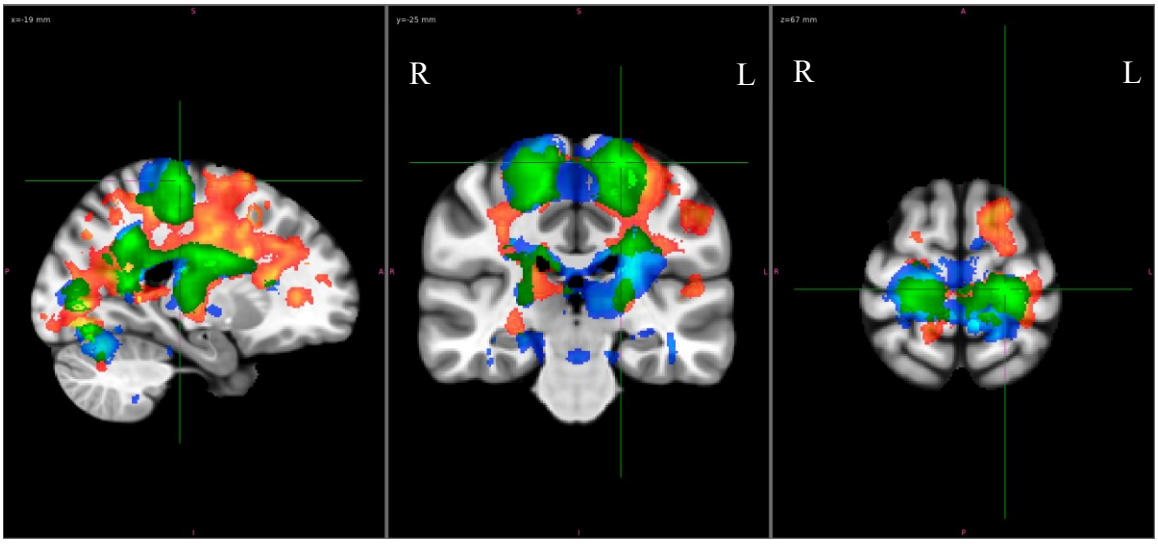

Figure 15. Conjoint analysis – negative BOLD signal correlates for the hedonic regressor (precentral gyrus). In blue: Hypothermia; in red: Hyperthermia; in green: Conjoint regions.

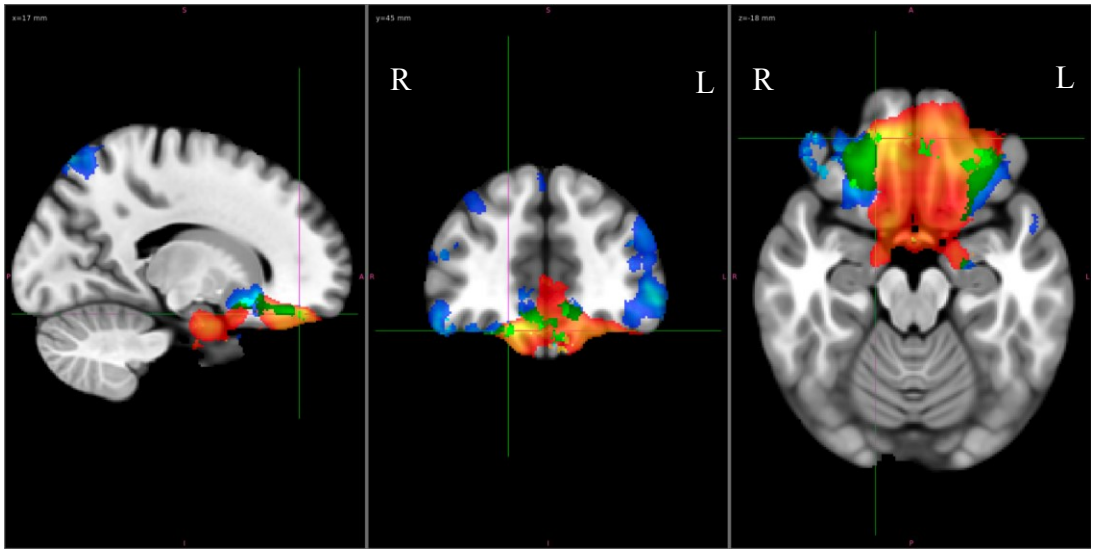

Figure 16. Conjoint analysis – positive BOLD signal correlates for the homeostatic regressor. In blue: Hypothermia; in red: Hyperthermia; in green: Conjoint regions.

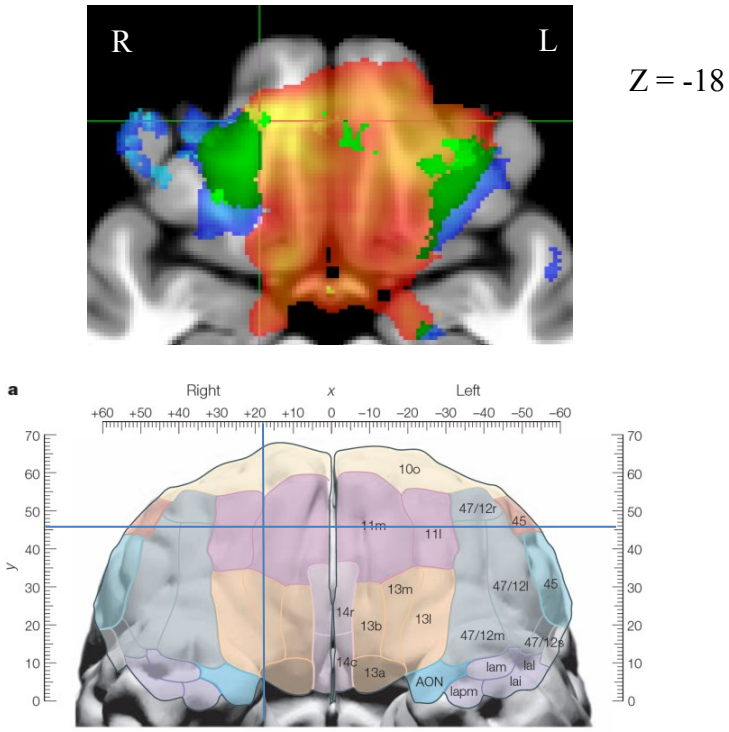

Figure 17. Localization of the orbitofrontal cortex homeostatic correlations with the cytoarchitectonic map established by Kringelbach (2005).

= -34, 4, -35, 4.92; cluster size = 2839 mm³) and in the frontal medial cortex (Peak: x, y, z, Z-value = -2, 47, -22, 4.55; cluster size = 1243 mm³). Figure 18 shows overlap between the present results and those obtained by Dunn et al. in parts of 11l, 11m, 13l, and 13m of the right orbitofrontal cortex. In the left hemisphere, the common region in the orbitofrontal cortex covered parts of 11l, 13l, 13m, and 47/12m.

Figure 19 shows the negative correlates for the homeostatic regressor which are found between the two thermal conditions. At the cortical level, the postcentral gyrus (Peak: x, y, z, Z-value = 2, -37, 65, 4.61; cluster size = 3785 mm³), the precentral gyrus (Peak: x, y, z, Z-value = 9, -21, 53, 3.26; cluster size = 1406 mm³), and the

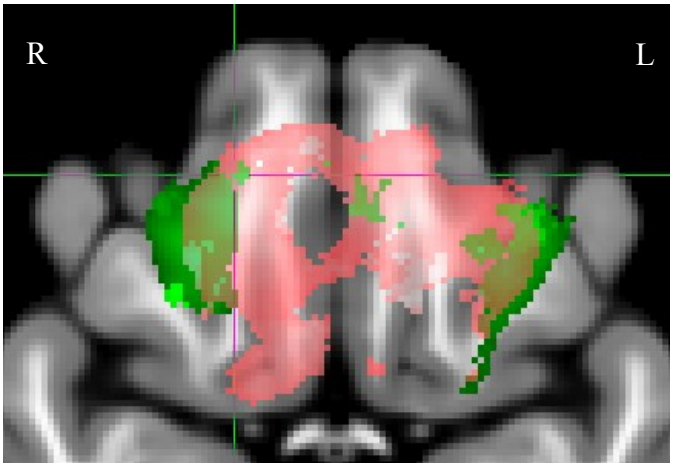

Figure 18. Conjoint analysis – comparison with Dunn et al.'s results for the homeostatic regressor. In green: Conjoint regions; in pink: Conjoint regions in Dunn et al.'s study.

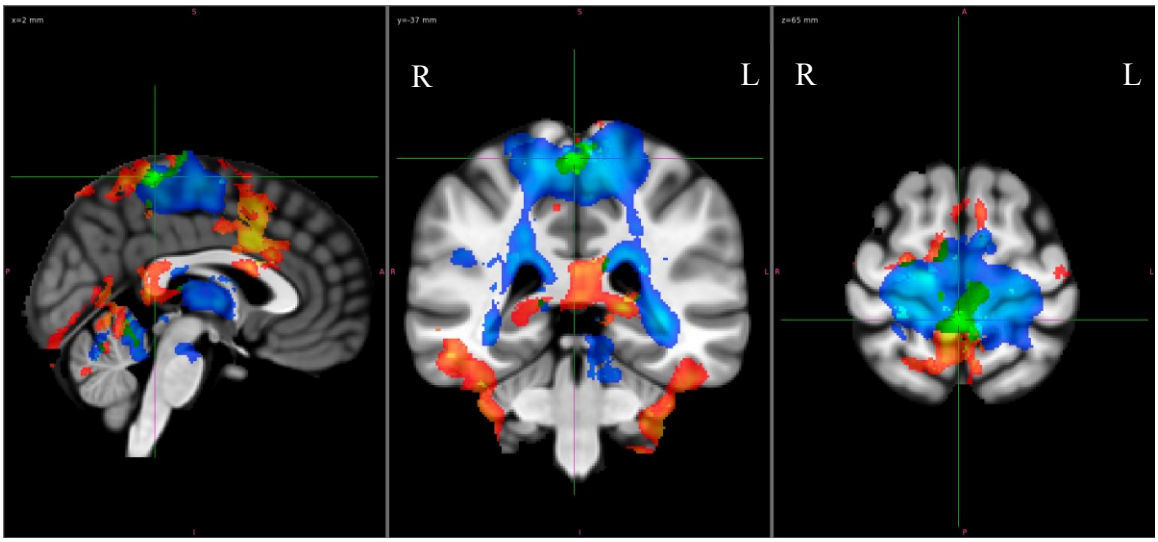

Figure 19. Conjoint analysis – negative BOLD signal correlates for the homeostatic regressor (postcentral gyrus). In blue: Hypothermia; in red: Hyperthermia; in green: Conjoint regions.

juxtapositional lobule cortex (Peak: x, y, z, Z-value = -10, -4, 52, 3.84; cluster size = 1380 mm^3) appear deactivated while at the subcortical level, the left and right thalamus (Peaks: x, y, z, Z-value = -22, -32, 7, 3.84; cluster size = 178; x, y, z, Z-value = 16, -35, 6, 2.71; cluster size = 50 mm^3), and the right caudate (Peak: x, y, z, Z-value = 16, 6, 20, 3.48; cluster size = 99 mm^3), appear deactivated.

The common regions between the two thermal conditions for the sensory regressor, in the case of the positive correlates, were more circumscribed. Clusters were found in the middle frontal gyrus (Peak: x, y, z, Z-value = -35, 2, 43, 4.09; cluster size = 1718 mm^3), the superior frontal gyrus (Peak: x, y, z, Z-value = -18, 11, 50, 3.06; cluster size = 284 mm^3), the precentral gyrus (Peak: x, y, z, Z-value = 35, 4, 30, 3.85; cluster size = 282 mm^3), and the orbitofrontal cortex (Peak: x, y, z, Z-value = 32, 26, -9, 2.77; cluster size = 254 mm^3) (Figure 20). The latter cluster (located in the right hemisphere at the border of 13l and 47/12m) was the only one that overlaps the clusters reported by Dunn et al.'s results (Figure 21). In the analysis of the negative correlates between the hyperthermia and hypothermia conditions, we found a single conjoint region: the right amygdala (Peak: x, y, z, Z-value = 10, -3, -17, 3.29; cluster size = 177 mm^3) (Figure 22).

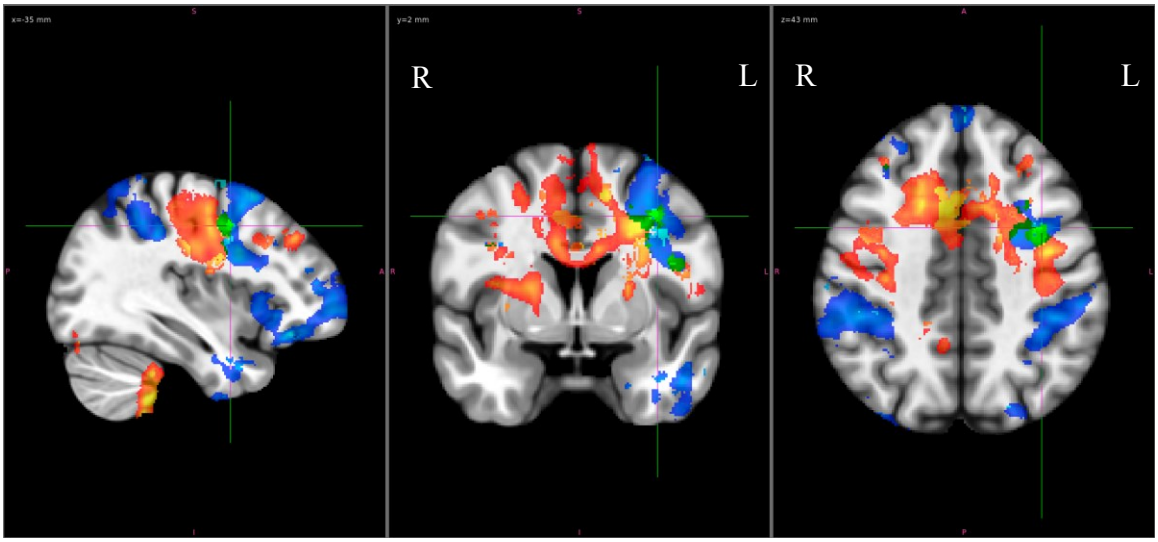

Figure 20. Conjoint analysis – positive BOLD signal correlates for the sensory regressor (lateral occipital cortex). In blue: Hypothermia; in red: Hyperthermia; in green: Conjoint regions.

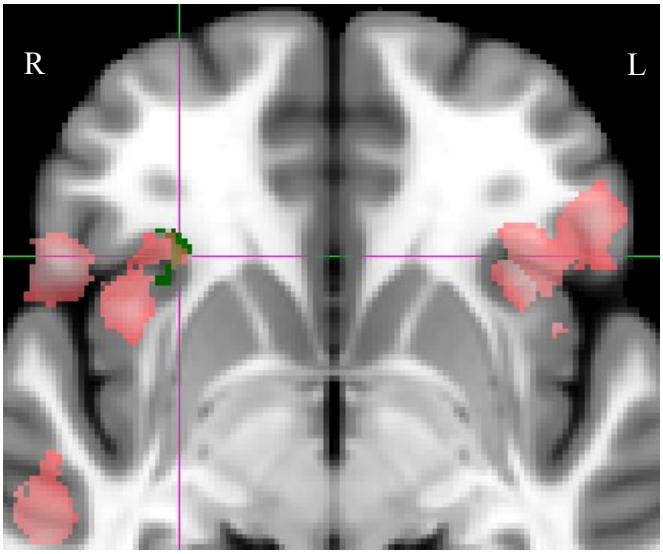

Figure 21. Conjoint analysis – comparison with Dunn et al.'s results for the sensory regressor (orbitofrontal cortex). In green: Conjoint regions; in pink: Conjoint regions in Dunn et al.'s study.

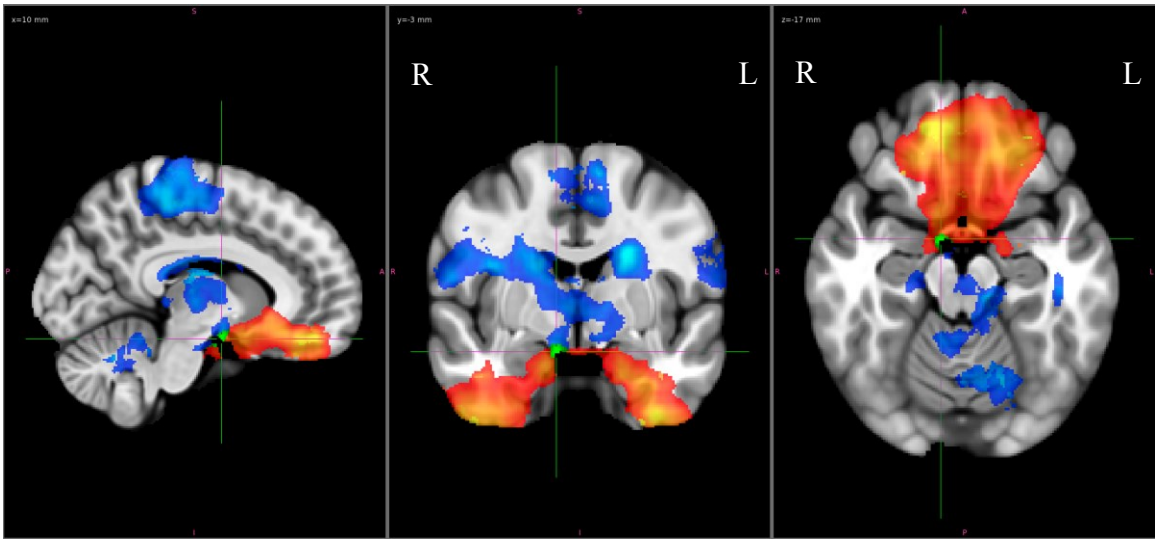

Figure 22. Conjoint analysis – negative BOLD signal correlates for the sensory regressor (right amygdala). In green: Conjoint regions; in pink: Conjoint regions in Dunn et al.'s study.

Finally, we performed a conjoint analysis to determine the regions in which common correlates of the hedonic and homeostatic regressors were seen both in this study and the one carried out by Dunn et al. Figure 23 shows overlapping regions in the lateral parts of the orbitofrontal cortex (in green, the conjoint cluster for the hedonic regressor; in yellow, the conjoint cluster for the homeostatic regressor; in blue, the conjoint cluster between these two regressors in Dunn et al.'s study). In the right hemisphere, the common region overlapped parts of 11l, 11m, and 13m. The small common cluster in the left hemisphere is located at the borders of 11l, 13l, and 13m.

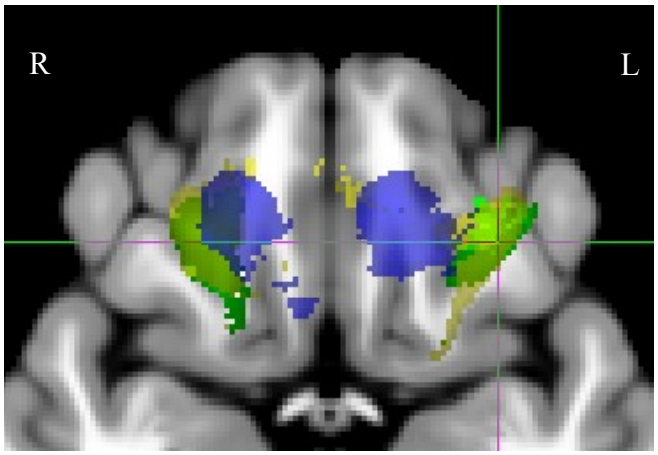

Figure 23. Comparison of the conjoint clusters for the hedonic and the homeostatic regressors between the current study and Dunn et al.'s study. In green and yellow are represented respectively the conjoint clusters of the hedonic and the homeostatic regressors for the current experiment. In blue are the conjoint clusters of Dunn et al.'s study for both the hedonic and the homeostatic regressors.

Discussion

In this experiment, we studied the brain correlates of hedonic value and sensation using the alliesthesia phenomenon. The initial core-temperature deviations (mild hyperthermia and hypothermia) and thermal stimulation over the whole body surface provided a unique context for studying hedonic and sensation encoding. As in the Dunn et al.'s experiment, we were able to compare brain activation patterns for two distinct thermal conditions. These two conditions differed only by the sequence of the trials with the first trial leading to an unpleasant feeling (i.e., hot water for hyperthermia and cold water for hypothermia). From the ratings of the participants on their subjective hedonic feelings (pleasantness/ unpleasantness) and sensory perceptions, we built three different regressor sets: hedonic, homeostatic, and sensory. As a result, we were able to distinguish brain correlates of hedonic value from those of sensation. For the hedonic and homeostatic regressor sets, the main results we obtained were activations in the OFC as reported by Rolls, Grabenhorst, and Parris (2008), and Dunn et al. (Unpublished thesis) for non-noxious thermal stimulations.

Interestingly, for both regressor sets we observed the same pattern of activation at the group level: a large activation covering the medial and lateral parts of the OFC for the hyperthermia condition, and circumscribed activations in the more lateral parts (of the medial and lateral areas of the OFC) for the hypothermia condition. Consequently, the conjoint activations are located more in the lateral parts of the OFC than in Dunn et al.'s results. Referring to the cytoarchitectonic map established by Kringelbach (2005), the common activations observed for each regressor sets cover parts of these areas: 11l, 11m,

13l, 13m, and 47/12m.

It has been proposed that the OFC is organized in one principal network, the orbital and medial prefrontal cortex (OMPFC) network, constituted by two specific and distinct networks: the orbital and the medial (Öngür and Price, 2000; Öngür, Ferry and Price, 2003; Kringelbach and Rolls, 2004; Kringelbach, 2005). The orbital network is composed mainly of the areas 11l, 13l, 13m, 47/12l, 47/12m, and 47/12s corresponding essentially to the activations observed in this study (Öngür, Ferry and Price, 2003). According to Kringelbach (2005), these areas would receive signals from sensory modalities, especially from the somatosensory cortex for the regions 13l and 47/12m which are both connected to the areas 11l and 13m (Figure 24). Öngür, Ferry and Price (2003) reported also that the orbital network could be involved with the appreciation and anticipation of rewards, which is consistent with our data. The medial network is principally constituted from the areas of the medial wall (10m, 10r, 10p, 24b, 25, and 32pl); Öngür, Ferry and Price (2003) suggest it is involved in visceral activity, notably in relation to affective stimuli. No clear conjoint activations were observed, despite the thermoregulation process involved. The two networks could be connected, especially through the areas 11m, 14c, and 14r (Öngür, Ferry and Price, 2003).

It has also been suggested that the hedonic encoding occurs in specific areas in the OFC, the medial part being associated notably to pleasantness (reward) and the lateral parts to unpleasantness (punishement) (Kringelbach and Rolls, 2004; Kringelbach, 2005; Murray, O'Doherty, and Schoenbaum, 2007; O'Doherty, 2007; Grabenhorst and Rolls, 2011). This dissociation has been observed with different types of stimuli in neuroimaging studies investigating correlates of odour (Rolls, Kringelbach and de

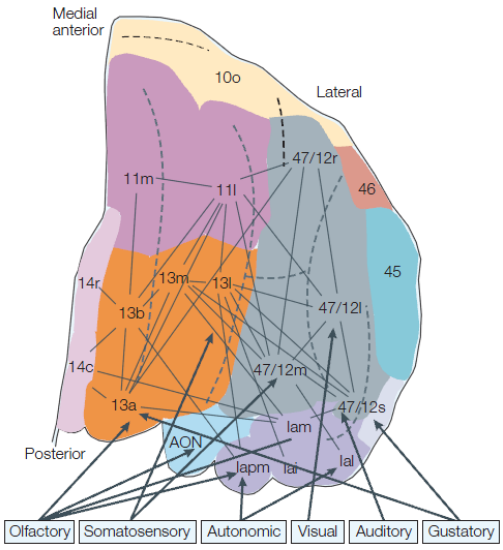

Figure 24. Schematic of the connectivity in the orbitofrontal cortex as established by Kringelbach (2005).

Araujo, 2003), money (O'Doherty et al., 2001), food (Small et al., 2003), facial expression (O'Doherty et al., 2003), and thermal stimuli (Rolls, Grabenhorst, and Parris, 2008; Dunn et al., 2010). Another dissociation has been proposed along the anterior-posterior axis in the OFC. It has been suggested that abstract or secondary reinforcers (i.e., money) are more likely to be processed in the anterior region of the OFC while primary reinforcers (i.e., erotic stimulation) would be processed in the posterior region (Sescousse, Redouté, and Dreher, 2010).

Our data corresponds to the medial (11 and 13), the lateral (47/12m), the anterior (11), and the posterior (13) areas of the OFC, partially reflecting the previous results. Thermal stimulations in this current experiment are clearly a primary reinforcer activating both the posterior and the anterior areas of the OFC. The specificity and/or the intensity of the stimulus could explain, in part, the disparity of the results. The stimuli of

seeing a picture of a sexy woman or winning a small amount of money as in the Sescousse, Redouté, and Dreher's study may be considered less rewarding than a thermal stimulation promoting return to normothermia, for instance.

To interpret the lateralization of the activations, we need to take into consideration that each regressor set was sensitive to the pleasant and unpleasant transitions (as measured by both ratings). In this sense, how could we explain the absence of a statistically significant activation in the more medial part of the orbitofrontal cortex for the hypothermia condition? Compared to Dunn et al.'s experiment that used a similar procedure, the current study differed mainly in the group of participants and the introduction of 'neutral' trials in the experimental design. The size and the composition of the samples may explain part of the variability of the results. The data of only 18 participants were analyzed in the current study (17 for the hyperthermia condition) compared to 16 in Dunn et al.'s experiment. In both cases, the samples are relatively small. We also recruited mainly young and lean athletes in-to-excellent physical condition (for instance, some participants were running about 100 kilometers per week) whereas Dunn et al.'s focused on more average fitness participants. The low body fat of the participants in the present study may have affected their hedonic valuation for the hypothermia condition. Since they were prevented from making gross movements in the scanner (thus reducing their ability to defend their core body temperature), this thermal condition may have been more challenging. Some participants did actually report after the experiment that the warm water trials were not pleasant or long enough and thus, less rewarding. The addition of the 'neutral' trials in the experimental design reduced the number of pleasant and unpleasant trials. This decreased the statistical power of the

analysis as compared to Dunn et al.'s experiment. In addition, the addition of the neutral trials reduced the number of large hedonic transitions (i.e., unpleasant to pleasant), which likely lessened the salience and rewarding effect of the changes in thermal stimulation.

Another element to take into consideration is the induction of hypothermia. For the majority of the participants, we relied exclusively on the tympanic thermometer to determine the ~one degree Celsius core body temperature deviation. Even with apparent shivering, the oral thermometer measurements indicated no significant deviation for nearly all the participants. It has been reviewed by Forbes et al. (2009) that the tympanic thermometer is the least reliable device for monitoring intraoperative temperatures of patients. Esophageal probes and oral thermometers are preferred. It has also been suggested by Rogers et al. (2007) that tympanic thermometers underestimate the core body temperature of swimmers in the state of hypothermia. Again, this study supports the reliability of oral thermometers. In our experiment, a participant near the state of normothermia would probably not appreciate both the cold and warm stimulations.

It is likely that the addition of the 'neutral' trials also reduced the contribution of anticipation. In Dunn et al.'s experiment, it is legitimate to think that the participants could eventually predict the trial sequence (unpleasant-pleasant) for the two thermal conditions. Moreover, in Dunn et al.'s experiment, since the structure for the hyperthermia and hypothermia conditions were analogous, the participants had presumably a better idea of what to expect in the second thermal condition. In the literature on anticipation in humans, it has been reported in some fMRI studies that the OFC was activated during the anticipation phase and during the receipt of the reward (O'Doherty et al., 2002; Kahnt et al., 2010). In addition, Nitschke et al. (2006) observed

activation in the OFC for aversive stimuli. Perhaps decreased anticipation explains, in part, the difference in the activation in the medial OFC noted in the two studies.

As for the sensory regressor, the main activations observed in the current experiment were in the middle frontal gyrus, the superior frontal gyrus, the precentral gyrus, and the orbitofrontal cortex. These results are interesting notably in regard to the study of Goldberg, Harel, & Malach (2006). In their fMRI experiment, brain correlates were compared as they occurred during a perceptual task and during self-reflective introspection. Goldberg, Harel, and Malach were also interested in distinguishing brain correlates of the self-related process involved in introspection from emotional processes. In a sense, their experiment has some resemblance to the current one. For the first part of the experiment, the participants were asked to categorize stimuli and to reflect on their emotional responses to the stimuli presented. Two sets of scans were performed for this block design experiment: one with visual stimuli (identifying animals among a series of pictures) and one with auditory stimuli (identifying the sound of trumpet among a series of sounds). For the introspection condition, the participants had to categorize their own reactions as high (positive or negative) or neutral. Among their results, the researchers observed brain activations in the prefrontal cortex (PFC) of the left hemisphere, in the superior frontal gyrus, in the middle frontal gyrus, and in the inferior frontal gyrus for the introspection condition. We noted similarities (the middle frontal gyrus and the superior frontal gyrus) with our sensory regressor results.

The second part of the experiment had some similarities to the first part in terms of the design. The participants were asked again to categorize stimuli and to do self-reflective introspection. In one of the three conditions, the 'semantic judgment',

participants had to categorize words (not emotionally charged) as either a noun or a verb. As for the two other conditions, the 'self-judgment' and the 'emotional picture judgment', participants had to respectively consider if they relied on the words presented (again, not emotionally charged) and if they judged positively or negatively the pictures shown. After their analyses, one of the main observations of Goldberg, Harel, and Malach was that the superior frontal gyrus seemed to be involved in the self-related process. In the context of our experiment, the water temperature perception in the state of hyperthermia/hypothermia could reflect the same self-reported process, explaining this activation.

Proposed improvements

This experiment could be improved in different ways. First, in spite of known thermal induction or technical difficulties, we included the data of four participants in the hyperthermia condition analysis. These four participants were the ones presenting inconsistent hedonic ratings to the alliesthesia predictions. For two participants (Hyper_he110822, and Hyper_he110718), we respectively lost the ~one degree Celsius core body temperature deviation prior to the scan, and we had to modify the induction procedure. In this specific case, the participant had to increase her effort intensity on the stationary bicycle significantly toward the end to reach the target deviation while respecting our time schedule. In contrast, the other participants had only to pedal slowly, and most of the heating occurred passively. The technical difficulties occurred in the scanning sessions of the participants Hyper_he12020, and Hyper_he120413. A problem with one of the hoses reduced the hot water flow, and a disconnected booster pump for the hot water altered the stimulations and thus, probably influenced the participants'

ratings. By scanning new participants to replace this data in the analysis, we would enhance the reliability of the results for the hyperthermia condition. As for the hypothermia condition, we previously mentioned issues regarding the core body temperature measurements. A better comprehension of both the processes involved in the induction of the hypothermia state, and the optimal functioning of the oral and tympanic thermometers would be beneficial. Also, an extra 30 minutes for the induction period would probably be helpful considering the constrained time schedule.

With the addition of the 'neutral' trials in the experimental design, we already highlighted the decrease of statistical power for the analysis as compared to Dunn et al. To overcome this concern, more participants should be tested. Moreover, there is a bias towards the 'bad' trials in the current design. The participants were exposed in total to four 'bad', three 'neutral', and three 'good' trials. Having an equivalent number of 'good' and 'bad' trials could be an adjustment to consider in a future experiment.

Future research

With the current experiment in mind, it would be interesting to study further how the brain encodes hedonic responses. Is it through a single- or dual-ended coding? In other words, is it a unique system encoding for both pleasant and unpleasant stimulations, or is it the combination of two distinct and specific systems encoding pleasant and unpleasant stimulations? Well established in colour vision, the idea of opponent processes, related to dual-ended coding, found echoes in motivation and hedonic states most notably through the work of Solomon (1974, 1980), and Seymour et al. (2005). The latter, inspired by Solomon's theoretical model, studied the opponent process in the case of pain specifically at the neuronal level. Based on the idea that a return to the

homeostatic state—after an imbalance—solicited reward processes, Seymour et al. defined pain relief as rewarding and pain exacerbation as penalizing. Using this framework, they did an fMRI experiment following a classical pavlovian delay-conditioning procedure in which the participants were presented a series of three distinct visual cues, each followed by a potentially predetermined stimulation (pain, pain relief, and control) induced by topical 1% capsaicin and thermode. The pain and the pain relief were, in fact, delivered 50% of the time. To evaluate the prediction errors and the corresponding brain activity, Seymour et al. employed the temporal difference learning model. They observed that two distinct neuronal patterns were activated in an opponent way for the two appetitive and aversive prediction errors defined. The blood-oxygenated-level dependent (BOLD) signal from the midbrain and the amygdala correlated with the appetitive prediction error signal. As for the aversive prediction error signal, it correlated with the BOLD signal from the lateral orbitofrontal cortex and anterior cingulate cortex. The time courses of the neurons involved in those two patterns appeared to be opponent. Based on Seymour et al.'s experiment, it appears that neurons within the significant clusters in those four distinct brain areas are probably of a double-ended type, at least regarding the encoding of those prediction errors. The 'neutral' trials in this current experiment could possibly facilitate finding evidence supporting either the single- or dual-ended coding of the hedonic response. We would essentially have to define regressor sets for the pleasant, unpleasant, and 'unique' system, and evaluate whether neurons, through the BOLD signal, are only activated or both activated and deactivated to the hedonic value of the stimulation. Generating the appropriate statistical maps and performing a conjoint analysis for the pleasant and unpleasant regressor sets could be a

way to determine the nature of the hedonic encoding.

A procedure developed by Shizgal, based on alliesthesia phenomenon, could also be interesting in studying the anticipation of the participants, notably their active role to forestall or delay stimulations. In the current experiment, all the participants were waiting passively for the next pleasant, unpleasant, or 'neutral' stimulation. In contrast, it has been reported notably by Tricomi, Delgado & Fiez (2004), and Delgado (2007) that the dorsal striatum is involved in the action leading to a reward or the avoidance of a punishment in humans. In an fMRI study, Tricomi, Delgado & Fiez (2004) did a series of three event-related experiments using an oddball paradigm. The three experiments were design to compare brain activation to rewards, to anticipation, and to action leading to a monetary outcome. In the first experiment, a series of three predetermined visual cues (arrows), associated with a definite gain, loss, or no money awarded, were presented pseudorandomly to the participants at intervals varying between 10,5 and 19,5 seconds. The participants had to press a button upon the presentation of the visual cues to get the corresponding money outcome. The second experiment differed from the first one, only by the elimination of the 'no money' trials and the addition of a new visual cue, a yellow circle; on 50% of the trials, the yellow circle appeared three seconds before the onset of the two remaining visual cues (arrows). Thus, the presentation of the yellow circle had no predictive value. In the third experiment, the yellow circle alternated randomly with a blue circle; one of the two circles appeared on half the trials three seconds before the onset of the two reward related arrows. The yellow circle led to a choice between two buttons to determine the monetary outcome. Each participant had to press one of two buttons before the onset of the arrow signaling a gain or loss. In contrast, the blue circle

led to a forced choice: the participants had been informed which button to press following presentation of the blue circle. Tricomi, Delgado, and Fiez principally reported significant activation in the caudate nucleus '…when the participants thought that their button presses determined whether they won or lost money; neither pseudorandomly presented rewards and punishments nor timelocked anticipation of the rewards and punishments was enough to drive such a response.' (Tricomi, Delgado & Fiez, 2004, p. 287)

The proposed experiment would differ from the current one, by presenting to the participants in the scanner the following information on a monitor: The water temperature of the following trial and the remaining time of its occurrence plus two Likert scales, presented in alternate order at 9 seconds intervals, related respectively to the participant's actual hedonic state and to the participant's desire to forestall or delay the upcoming trial. By pressing a button box, the participants would have the possibility to actually forestall or delay the next trial allowing us to measure objectively that desire. It would then be possible, with the appropriate regressor, to determine at the group level the brain correlates associated to that desire. By comparing the result with the brain correlates related to the hedonic evaluation, we would be able to distinguish the two processes.

Conclusion

The present experiment provides further evidence linking the orbitofrontal cortex (OFC) to hedonic valuation. The experimental protocol, and the alliesthesia phenomenon on which it is based, made it possible to distinguish between hedonic correlates of activity in different OFC regions. Whereas activations in the medial part of the OFC were associated with pleasantness, activations in the lateral part were associated with unpleasantness. That said, the dissociation was clearest in the hyperthermia condition; in the hypothermia condition, more lateral activations were observed even in response to 'pleasant' stimulation provided by the flow of hot water through the suit. The experiment of Dunn and colleagues made use of a similar protocol but yielded results in the hypothermia conditions that are more consistent with alliesthesia. This discrepancy may reflect several differences between the present study and that of Dunn et al., including the introduction of 'neutral' trials, the level of fitness of the participants, and the magnitude of the core-temperature deviations.

Experimental protocols based on the alliesthesia phenomenon provide promising tools for the study of decision making at the neurological level. The essence of these protocols is the distinction they provide between the correlates of sensory and hedonic experience. No other strategy has been proposed to make such a distinction. The present experiment provides qualified support for the validity of the alliesthesia-based approach.

Thermal stimuli are powerful primary reinforcers, and the responses to them are critical for homeostasis and survival. Future work can reveal the degree to which the results obtained using these stimuli can be generalized to the neural processing of other

hedonically potent and biologically important stimuli. Decisions about whether to approach or avoid a goal object and whether to maintain or break off contact are characterized ultimately by only a single degree of freedom. Thus, it stands to reason that there is a final common path in the nervous system through which the myriad factors contributing to approach/withdrawal decisions are funnelled. If so, the neural circuitry that processes the hedonic impact of thermal stimuli should be expected to share important components with the neural substrates for other determinants of hedonic experience.

References

Beckmann, C., Jenkinson, M., & Smith, S. (2003). General multilevel linear modeling for group analysis in FMRI. *NeuroImage, 20*, 1052-1063.

Beckmann, C., & Smith, S. (2004). Probabilistic independent component analysis for functional magnetic resonance imaging. *Medical Imaging, IEEE Transactions on Medical Imaging, 23(2)*, 137-152.

Cabanac, M. (1971). Physiological role of pleasure. *Science, 173(4002),* 1103-1107.

Cabanac, M. (1979). Sensory pleasure. *Quarterly Review of Biology, 54*, 1-29.

Center for Brain Science (n.d.). Basic MRI physics and protocol questions. Retrieved from http://cbs.fas.harvard.edu/science/core-facilities/neuroimaging/information-investigators/MRphysicsfaq.

Deichman, R., Gottfried, J.A., Hutton, C., & Turner, R. (2003). Optimized EPI for fMRI studies of the orbitofrontal cortex. *NeuroImage, 19*, 430-441.

Delgado, M. (2007). Reward-related responses in the human striatum. *Annals of the New York Academy of Sciences, 1104*, 70-88.

Dunn, B.J., Conover, K., Plourde, G., Munro, D., Kilgour, R., & Shizgal, P. An fMRI study of human hedonic valuation during thermal alliesthesia. Poster presented at the 16th annual meeting of the Organization for Human Brain Mapping, Barcelona, Spain, June 7-8, 2010, OHBM on-line Itinerary Planner, Poster 629 MT-AM.

Dunn, B.J. (2010). *Human hedonic experience during thermal alliesthesia: a functional magnetic resonance imaging study*. Unpublished master's thesis, Concordia University, Montreal, Canada.

Elliott, R., Agnew, Z., & Deakin, J.F.W. (2010). Hedonic and informational functions of the human orbitofrontal cortex. *Cerebral Cortex, 20*, 198-204.

Farrell, M.J., Johnson, J., McAllen, R., Zamarripa, F., Denton, D.A., Fox, P.T., & Egan, G.F. (2011). Brain activation associated with ratings of the hedonic component of thermal sensation during whole-body warming and cooling. *Journal of Thermal Biology*, *36*, 57-63.

Forbes, S.S., Eskicioglu, C., Nathens, A.B., Fenech, D.S., Laflamme, C., & McLean, R.F. (2009). Evidence-based guidelines for prevention of perioperative hypothermia. *Journal of the American College of Surgeons, 209(4)*, 492-503.

Goldberg, I.I., Harel, M., & Malach, R. (2006). When the brain loses its self: prefrontal inactivation during sensorimotor processing. *Neuron, 50*, 329-339.

Grabenhorst, F., & Rolls, E.T. (2009). Different representations of relative and absolute subjective value in the human brain. *NeuroImage, 48(1)*, 258-268.

Grabenhorst, F., & Rolls, E.T. (2011). Value, pleasure and choice in the ventral prefrontal cortex. *Trends in Cognitive Sciences, 15(2)*, 56-67.

Jenkinson, M., Bannister, P., Brady, M., & Smith, S. (2002). Improved optimization for the robust and accurate linear registration and motion correction of brain images. *NeuroImage, 17*, 825-841.

Jenkinson, M., Pechaud, M., & Smith, S. (2005). BET2: MR-based estimation of brain, skull and scalp surfaces. In Eleventh Annual Meeting of the Organization for Human Brain Mapping, 2005.

Kahnt, T., Heinzle, J., Park, S.Q., & Haines, J.D. (2010). The neural code of reward anticipation in human orbitofrontal cortex. *Proceedings of the National Academy of Sciences of the United States of America, 107(13)*, 6010-6015.

Kringelbach, M.L. (2004). Food for thought: hedonic experience beyond homeostasis in the human brain. *Neuroscience, 126*, 807-819.

Kringelbach, M.L. (2005). The human orbitofrontal cortex: linking reward to hedonic experience. *Nature Reviews Neuroscience, 6*, 691-702.

Kringelbach, M.L., & Rolls, E.T. (2004). The functional neuroanatomy of the human orbitofrontal cortex: evidence from neuroimaging and neuropsychology. *Progress in Neurobiology, 72,*341-372.

Kringelbach, M.L., & Berridge, K.C. (2010). The functional neuroanatomy of pleasure and happiness. *Discovery Medicine, 9(49),* 579-587.

Murray, E.A., O'Doherty, J.P., & Schoenebaum, G. (2007). What we know and do not know about the functions of the orbitofrontal cortex after 20 years of cross-species studies. *Journal of Neuroscience, 27(31),* 8166-8169.

Nitschke, J.B., Sarinopoulos, I., Mackiewicz, K.L., Schaefer, H.S., & Davidson, R.J. (2006). Functional neuroanatomy of aversion and its anticipation. *NeuroImage, 29*, 106–114.

O'Doherty, J., Kringelbach, M.L., Rolls, E.T., Hornak, J., & Andrews, C. (2001). Abstract reward and punishment representations in the human orbitofrontal cortex. *Nature Neuroscience, 4*, 95-102.

O'Doherty, J.P., Deichmann, R., Critchley, H.D., & Dolan, R.J. (2002). Neural responses during anticipation of a primary taste reward. *Neuron, 33*, 815–826.

O'Doherty, J., Winston, J., Critchley. H., Perrett, D., Burt, D.M., Dolan, R.J. (2003). Beauty in a smile: the role of medial orbitofrontal cortex in facial attractiveness. *Neuropsychologia, 41(2)*, 147-155.

O'Doherty, J.P. (2007). Lights, camembert, action! The role of human orbitofrontal cortex in encoding stimuli, rewards, and choices. *Annals of the New York Academy of Sciences, 1121,* 254-272.

Olson, I.R., Plotzker, A., & Ezzyat, Y. (2007). The enigmatic temporal pole: a review of findings on social and emotional processing. *Brain, 130*, 1718-1731.

Öngür, D., & Price, J.L. (2000). The organization of networks within the orbital and medial prefrontal cortex of rats, monkeys and humans. *Cerebral Cortex, 10(3)*, 206-219.

Öngür, D., Ferry, A.T., & Price, J.L. (2003). Architectonic subdivision of the human orbital and medial prefrontal cortex. *The Journal of comparative neurology, 460*, 425-449.

Rogers, I.R., Brannigan, D., Montgomery, A., Khangure, N., Williams, A., & Jacobs, I. (2007). Tympanic thermometry is unsuitable as a screening tool for hypothermia after open water swimming. *Wilderness and Environmental Medicine, 18(3)*, 218-221.

Rolls, E.T., Grabenhorst, F., & Parris, B. (2008). Warm pleasant feelings in the brain. *NeuroImage, 41*, 1504-1513.

Rolls, E.T., Kringelbach, M.L., & De Araujo, I.E.T. (2003). Different representations of pleasant and unpleasant odours in the human brain. *European Journal of Neuroscience, 18 (3),* 695-703.

Sescousse, G., Redouté, J., & Dreher, J-C. (2010). The architecture of reward value coding in the human orbitofrontal cortex. *The Journal of Neuroscience, 30(39)*, 13095-13104.

Seymour, B., O'Doherty, J.P., Koltzenburg, M., Wiech, K., Frackowiak, R., Friston, K., & Dolan, R. (2005). Opponent appetitive-aversive neural processes underlie predictive learning of pain relief. *Nature Neuroscience, 8(9)*, 1234-1240.

Shizgal, P., Conover, K., Dunn, B., Munro, D., Kilgour, R., & Plourde, G. Neural correlates of thermal comfort and discomfort in humans: functional magnetic resonance imaging. Program No. 882.15. 2008 Abstract Viewer/Itinerary Planner. Washington, DC: Society for Neuroscience, 2008. Online.

Small, D.M., Gregory, M. D., Mak, Y. E., Gitelman, D., Mesulam, M.-M., & Parrish, T. (2003). Dissociation of neural representation of intensity and affective valuation in human gustation. *Neuron, 39*, 701-711.

Smith, S. (2002). Fast robust automated brain extraction. *Human Brain Mapping, 17(3),* 143-155.

Smith, S., Jenkinson, M., Woolrich, M., Beckmann, C., Behrens, T., Johansen-Berg, H., et al. (2004). Advances in functional and structural MR image analysis and implementation as FSL. *NeuroImage, 23*, S208-S219.

Solomon, R.L., & Corbit, J.D. (1974). An Opponent-process theory of motivation: I. temporal dynamics of affect. *Psychological Review, 81(2),* 119–145.

Solomon, R.L. (1980). The opponent-process theory of acquired motivation: the costs of pleasure and the benefits of pain. *American Psychologist, 35(8),* 691–712.

Tricomi, E.M., Delgado, M.R., & Fiez, J.A. (2004). Modulation of caudate activity by action contingency. *Neuron, 41*, 281-292.

Woolrich, M.W., Behrens, T.E.J., Beckmann, C.F., Jenkinson, M., & Smith, S.M. (2004). Multilevel linear modelling for FMRI group analysis using Bayesian inference. *NeuroImage, 21*, 1732-1747.